

1 *Bifidobacterium longum* modifies a nutritional intervention for stunting in Zimbabwean infants

2 Authors: Ethan K Gough<sup>1,\*</sup>, Thaddeus J Edens<sup>2</sup>, Lynnea Carr<sup>3</sup>, Ruairi C Robertson<sup>4</sup>, Kuda Mutasa<sup>5</sup>, Robert  
3 Ntozini<sup>5</sup>, Bernard Chasekwa<sup>5</sup>, Hyun Min Geum<sup>6</sup>, Iman Baharmand<sup>6</sup>, Sandeep K Gill<sup>6</sup>, Batsirai Mutasa<sup>5</sup>,  
4 Mduduzi N N Mbuya<sup>5,7</sup>, Florence D Majo<sup>5</sup>, Naume Tavengwa<sup>5</sup>, Freddy Francis<sup>8</sup>, Joice Tome<sup>5</sup>, Ceri  
5 Evans<sup>4,5,9</sup>, Margaret Kosek<sup>10</sup>, Andrew J Prendergast<sup>4,5</sup>, Ameer R Manges<sup>6,11</sup> for the Sanitation Hygiene  
6 Infant Nutrition Efficacy (SHINE) Trial Team.

7 Affiliations:

8 <sup>1</sup>Department of International Health, Johns Hopkins Bloomberg School of Public Health, Baltimore, MD,  
9 21205, USA.

10 <sup>2</sup>Devil's Staircase Consulting, West Vancouver, BC, Canada.

11 <sup>3</sup>Department of Microbiology and Immunology, University of British Columbia, Vancouver, BC, V6T 1Z3,  
12 Canada.

13 <sup>4</sup>Blizard Institute, Queen Mary University of London, London, E1 2AT, UK.

14 <sup>5</sup>Zvitambo Institute for Maternal and Child Health Research, Harare, Zimbabwe.

15 <sup>6</sup>School of Population and Public Health, University of British Columbia, Vancouver, BC, V6T 1Z3, Canada.

16 <sup>7</sup>Global Alliance for Improved Nutrition, Washington, DC, 20036, USA.

17 <sup>8</sup>Department of Experimental Medicine, University of British Columbia, Vancouver, BC, V6T 1Z2, Canada.

18 <sup>9</sup>Department of Clinical Infection, Microbiology and Immunology, University of Liverpool, Liverpool, L69  
19 3BX, UK

20 <sup>10</sup>University of Virginia School of Medicine, Charlottesville, VA, USA.

21 <sup>11</sup>British Columbia Centre for Disease Control (BCCDC), Vancouver, BC, Canada.

22 \*Correspondence: [egough1@jh.edu](mailto:egough1@jh.edu)

23

24

25

26

27

28

29

30

31

32

33

34

35

36

37

38

39

40 **Summary**

41 Child stunting is an indicator of chronic undernutrition and reduced human capital. Small-quantity lipid-  
42 based nutrient supplements (SQ-LNS) has been widely tested to reduce stunting, but has modest effects.  
43 The infant intestinal microbiome may contribute to stunting, and is partly shaped by mother and infant  
44 histo-blood group antigens (HBGA). We investigated whether mother-infant fucosyltransferase status,  
45 which governs HBGA, and the infant gut microbiome modified the impact of SQ-LNS on stunting at age  
46 18 months among Zimbabwean infants in the SHINE Trial (NCT01824940). We found that mother-infant  
47 fucosyltransferase discordance and *Bifidobacterium longum* modified SQ-LNS efficacy. Infant age-related  
48 microbiome shifts in *B. longum* subspecies dominance from *infantis*, a proficient human milk  
49 oligosaccharide utilizer, to *suis* or *longum*, proficient plant-polysaccharide utilizers, were partly  
50 influenced by discordance in mother-infant FUT2+/FUT3- phenotype, suggesting that a “younger”  
51 microbiome at initiation of SQ-LNS reduces its benefits on stunting in areas with a high prevalence of  
52 linear growth restriction.

53

54 Keywords: microbiome, nutrition, fucosyltransferase, histo-blood group antigen, stunting, infant

55

56

57

58

59

60

## 61 Introduction

62 Globally, 21% of children under 5 years of age (149 million) are stunted<sup>1</sup>, defined as having a length  
63 or height >2 standard deviations below an age- and sex-matched reference population median<sup>2</sup>. Deficits  
64 in linear growth largely accrue from conception to 24 months of age<sup>3,4</sup>, corresponding to the period  
65 when normal child growth and development is most rapid. Stunting is associated with reductions in child  
66 survival, neurodevelopment, educational attainment, and adult economic productivity<sup>5-7</sup>.

67 A broadly tested intervention to reduce stunting has been provision of small-quantity lipid-based  
68 nutrient supplements (SQ-LNS) to improve infant and young child feeding (IYCF) starting at 6-months  
69 (mo) of age, which is the recommended time for introduction of complementary foods. Randomized  
70 controlled trials (RCT) of SQ-LNS provision to infants have shown small reductions in stunting (12%  
71 relative reduction), but effects have varied<sup>8,9</sup>. Evidence to support other nutrition interventions, which  
72 address the underlying determinants of stunting during the first 1000 days of life, starting from  
73 conception, is also limited<sup>10</sup>. Elucidating the reasons for the limited impact of nutritional interventions  
74 that are designed to alleviate stunting is crucial to the development of more effective strategies.

75 Recently, the human microbiome has been shown to impact infant health<sup>11</sup>, and studies suggest a  
76 role of the intestinal microbiome in child growth, particularly ponderal growth<sup>12,13</sup>. The prevailing view  
77 holds that intestinal colonization with bacteria begins at birth, after which the microbiome progresses  
78 through a succession of identifiable shifts in composition and functional capacity<sup>11</sup> that correspond  
79 closely with infant age and developmental stage<sup>14</sup>. Deviations from an age-appropriate composition may  
80 be associated with poor health outcomes<sup>14-17</sup>, including undernutrition in low resource settings<sup>14,18-20</sup>.  
81 However, results vary<sup>21-25</sup> and evidence for a causal effect of the intestinal microbiome on growth  
82 comes predominantly from animal models. In these experiments, a combination of commensal bacteria  
83 and a nutrient-poor diet produce a synergistic effect on growth faltering. The detrimental effect on



84 growth was worse when certain commensal bacteria, which can act as pathobionts (e.g. *Bacteroides*  
85 *thetaiotaomicron* and *Bacteroides fragilis*), were present in the gut along with pathogenic species<sup>26,27</sup>.

86 The gut microbiome in infants is influenced by breastfeeding, with differences persisting beyond age  
87 6mo<sup>16</sup>. Breastfeeding-associated differences are partly driven by differences in human milk  
88 oligosaccharide (HMO) composition, which are metabolized by specific commensal bacteria and thereby  
89 influence the growth and activity of bacterial populations in the infant gut, in particular,  
90 *Bifidobacterium*<sup>28,29</sup>. In addition, HMOs in combination with commensal gut bacteria have been shown  
91 to improve growth in animal models of undernutrition<sup>30</sup>. Active maternal  $\alpha$ -1,2-fucosyltransferase  
92 (FUT2) and  $\alpha$ -1,3-fucosyltransferase (FUT3) genes are key determinants of HMO composition<sup>31-33</sup>. These  
93 genes encode enzymes which catalyze addition of fucose to the disaccharides that serve as precursors to  
94 host glycan production<sup>34,35</sup>. Individuals with at least one functional FUT2 or FUT3 allele produce  
95 fucosylated histo-blood group antigens (HBGA) and are called “secretors” or “Lewis-positive”,  
96 respectively;<sup>35</sup> by contrast, individuals lacking two functional FUT2 or FUT3 alleles don’t produce  
97 fucosylated HBGAs, and are termed “non-secretors” or “Lewis-null”, respectively<sup>35</sup>. These secretor and  
98 Lewis phenotypes act in concert to synthesize a variety of HBGAs (Figure S1)<sup>34,35</sup>. In addition to the  
99 impact of maternal FUT2 or FUT3 status on the infant gut microbiome via their influence on HMO  
100 composition, host FUT2 and FUT3 phenotypes also determine tissue surface HBGA expression in the gut,  
101 which may also affect the microbiome through the availability host glycans and competition for  
102 adhesion sites<sup>36-40</sup>.

103 There is growing interest in the moderating effect of the gut microbiome on nutritional  
104 interventions. Recent RCTs showed that the impact of dietary interventions for weight reduction on  
105 metabolic health outcomes is modified up to 4-fold by microbiota composition<sup>41-44</sup>. Effect modification  
106 of host diet by the gut microbiota has also been investigated in observational studies, which report that  
107 microbiome composition modified the association between diet and biomarkers of metabolic syndrome

108 by up to 2-fold<sup>45-47</sup>. Gut microbiota composition, therefore, may also be an important modifier of dietary  
109 interventions on infant health. Only one study to date investigated the gut microbiota as an effect  
110 modifier of SQ-LNS on infant stunting, and reported limited evidence of effect-modification<sup>48</sup>. However,  
111 several studies have reported a synergistic effect of microbiome composition and diet on undernutrition  
112 phenotypes using animal models<sup>26,27,49,50</sup>.

113 Here we aimed to determine the effect of infant gut microbiome composition and functional  
114 capacity on efficacy of an IYCF intervention that included SQ-LNS to reduce stunting (primary outcome)  
115 and improve length-for-age z-score (LAZ) (secondary outcome) at age 18mo. We hypothesized that the  
116 efficacy of IYCF, when started at age 6mo, on infant linear growth is modified by mother and infant FUT2  
117 and FUT3 phenotype, as an drivers of variation in gut microbiome composition, and by the infant gut  
118 microbiome. We tested this hypothesis using data from HIV-unexposed infants enrolled in the Sanitation  
119 Hygiene Infant Nutrition Efficacy (SHINE) trial conducted in rural Zimbabwe, in which the IYCF  
120 intervention modestly increased LAZ by 0.16 standard deviations and reduced stunting by 20% at age  
121 18mo<sup>51</sup>. We found that mother-infant FUT2 and FUT3 phenotype, where the mother was FUT2+/FUT3-  
122 but the infant was not, was associated with greater IYCF reduction of stunting at 18mo. Greater impact  
123 of IYCF on stunting was also associated with infant microbiome species maturation, characterized by a  
124 shift away from *Bifidobacterium longum* carriage. *B. longum*-dominant microbiome composition was  
125 characterized by *B. longum* strains that were most similar to subspecies *infantis*, a proficient HMO  
126 utilizer. In addition, *B. longum* abundance and odds of detecting different *B. longum* strains were  
127 explained by infant age and differences between mother-infant pairs in FUT2+/FUT3- phenotype.

128

129

130

131

132 **Results**

133 *Mother-infant FUT2+/FUT3- phenotype discordance modifies the effect of IYCF on stunting at 18mo*

134 In a substudy of the SHINE trial, we assessed FUT2 and FUT3 status in mothers and infants from  
135 saliva samples. To determine the impact of maternal and infant HBGA on IYCF efficacy, we investigated  
136 whether concordance in secretor (FUT2) and Lewis (FUT3) phenotypes between mother and infant pairs  
137 modified the effect of IYCF on stunting or LAZ at 18mo. We defined these paired mother-infant  
138 phenotypes using combinations of FUT2 and FUT3 status (as presented in Table S1) to more precisely  
139 reflect the potential for joint activity of these enzymes in HBGA production (as presented in Figure S1).  
140 Each of these paired mother-infant FUT2/FUT3 phenotypes were classified as *both* (if mother and infant  
141 shared the same phenotype), *none* (if neither had the phenotype), *infant only* (if the infant had the  
142 phenotype but the mother did not) or *mother only* (if the infant did not have the phenotype but the  
143 mother did). We fitted multivariable regression models that included terms for the interaction of IYCF  
144 and each paired FUT2/FUT3 phenotype between mother and infant, as well as prespecified covariates  
145 from the 6mo follow-up visit when IYCF was started, with stunting status at the 18mo visit as the  
146 dependent variable. We fitted separate models for each combination of paired mother-infant  
147 FUT2/FUT3 phenotype presented in Table S1 and Figure S1. These models were restricted to 792 infants  
148 who had both maternal and infant FUT2 and FUT3 status ascertained (Figure S2). Analyses were  
149 repeated with LAZ at the 18mo visit as the dependent variable.

150 Amongst infants who were randomized to IYCF, those who were in the *mother only* FUT2+/FUT3-  
151 group (13.5%) had a probability of stunting at 18mo that was -33.0% lower (95%CI:-55.0%,-10.0%) than  
152 infants in the *both* FUT2+/FUT3- group (11.1%) (Table 1). The *infant only* (11.1%) and *none* (64.3%)  
153 FUT2+/FUT3- groups, and other mother-infant FUT2 and FUT3 phenotype combinations (Table S1,  
154 Figure S1), did not show evidence of effect modification of IYCF on stunting (Table S2), and there was no  
155 evidence of effect modification on LAZ at 18mo after FDR-adjustment for multiple testing (Table S3).

156 Overall, our results indicate that discordance between mothers and infants in the FUT2+/FUT3-  
157 phenotype, whereby mothers had the phenotype and infants didn't have the phenotype, was associated  
158 with increased efficacy of IYCF to reduce stunting but not to increase LAZ.

159

160 *Infant gut microbiome composition modifies the effect of the IYCF intervention on stunting at 18mo*

161 Given our finding that infants whose mothers were FUT2+/FUT3-, while the infant was not, had  
162 greater reductions in stunting by IYCF; and considering the potential importance of FUT2/FUT3  
163 phenotypes on early infant microbiome composition via variation in maternal HMO composition and  
164 infant gut epithelial HBGA expression, we investigated whether infant gut microbiota species maturation  
165 showed evidence for modification of IYCF efficacy on stunting or LAZ at 18mo. First, we used 354 infant  
166 metagenomes from 172 infants collected from 1-18mo of age to fit a constrained Principal Coordinates  
167 Analysis (PCoA) model that included infant age at stool collection and three dummy variables for  
168 mother-infant FUT2+/FUT3- status representing the *none*, *infant only*, and *mother only* groups with the  
169 *both* group as the referent (see next section for details). Thus, we derived four PCoA axis scores from  
170 this model representing variation in microbiome composition due to infant age and explained by *none*,  
171 *infant only*, or *mother only* FUT2+/FUT3- status compared to *both*. Next, we fitted a multivariable  
172 regression model that included an IYCF-by-PCoA axis 1 score interaction term and prespecified  
173 covariates. The regression model was restricted to 53 infants who had a fecal specimen collected at the  
174 6mo follow-up visit when IYCF started and used their covariate values at the 6mo visit (Figure S2).  
175 Stunting status at 18mo was used as the dependent variable. We repeated our analyses using PCoA axis  
176 2 to 4 scores. Finally, we fitted regression models replacing stunting status with LAZ at 18mo as the  
177 dependent variable.

178 Greater PCoA axis 1 scores represented species turnover with increasing infant age (Figure S3), thus  
179 reflecting microbiota maturation, while greater PCoA axis 2 scores represented changes in species

180 composition associated with mother-infant FUT2+/FUT3- phenotypes (Figure S3). PCoA axis 1 and 2  
181 scores showed evidence of interaction with IYCF on stunting at 18mo (Table 2), but not LAZ (Table S4).  
182 Amongst infants randomized to IYCF, those with higher PCoA axis 1 scores at age 6mo were less likely to  
183 be stunted at 18mo compared to infants with lower PCoA axis 1 scores (difference-in-differences -76.0%  
184 [95%CI: -99.0%,-32.0%, adjusted p=0.003) (Table 2). In contrast, infants randomized to IYCF with higher  
185 PCoA axis 2 scores at age 6mo were more likely to be stunted at 18mo compared to infants who had  
186 lower PCoA axis 2 scores (difference-in-differences, 14.0% [95%CI: 7.0%,21.0%], adjusted p=0.001)  
187 (Table 2). Taken together, our findings showed that infant age-related microbiome species maturation  
188 was associated with greater reduction in the probability of stunting at 18mo by IYCF, indicating greater  
189 efficacy of the intervention; while microbiome species composition related to mother-infant  
190 FUT2+/FUT3- phenotype was associated with lesser reduction in stunting, suggesting variation in  
191 microbiome composition due to these infant characteristics is an important determinant of SQ-LNS  
192 efficacy to reduce stunting.

193  
194 *Infant age and mother-infant FUT2+/FUT3- phenotype explain shifts in microbiome species composition,*  
195 *in particular, Bifidobacterium longum*

196 To investigate sources of variation in infant intestinal microbiome composition and derive  
197 interpretable measures of species turnover, we performed constrained PCoA of Bray-Curtis  
198 dissimilarities with permutational analysis of variance using distance matrices for hypothesis testing.  
199 Infant age at stool collection explained 12.6% (ADONIS2 p=0.001) of the variability in microbiome  
200 composition (Table S5). Notably, exclusive breastfeeding (EBF) at 3mo was not significantly associated  
201 ( $R^2=0.346$ , ADONIS2 p=0.483) with microbiome composition (Table S5). However, 93.2% of mothers in  
202 these analyses reported exclusive breastfeeding (Table S6). Thus, there may not have been sufficient  
203 variability in infant breastfeeding practices in this cohort to identify EBF-associated differences between

204 infant microbiomes. Also, inclusion of specimens collected throughout the follow-up period in our PCoA  
205 models may have obscured associations with EBF, since EBF is only recommended up to age 6mo.

206 We then fitted a fully adjusted multivariable constrained PCoA model that included both infant age  
207 at stool collection and mother-infant FUT2+/FUT3- phenotype. We retained the latter variable to  
208 capture variation in microbiota composition associated with mother-infant FUT2+/FUT3- status after  
209 controlling for infant age, because of our *a priori* aim to investigate whether microbiome variation due  
210 to mother and infant FUT2/FUT3 phenotype was a modifier of the IYCF intervention, and our finding  
211 that the *mother only* FUT2+/FUT3- group was associated with a modified intervention effect. In the full  
212 model, age explained 12.8% (ADONIS p=0.001) and mother-infant FUT2+/FUT3- phenotype explained  
213 0.81% (ADONIS p=0.323) of the variation in microbiome composition (Table S5), indicating that infant  
214 age was the main driver of microbiome-wide changes in species composition in this cohort.

215 Age-related maturation in species composition were characterized by decreased relative abundance  
216 of *B. longum*, and increased relative abundance of *Prevotella copri*, *Faecalibacterium prausnitzii*, *Dorea*  
217 *longicatena*, and *Dorea formicigenerans* (Figure S4). Mother-infant FUT2+/FUT3- discordance was  
218 characterized by increased relative abundance of *B. longum* in the *none* and *infant only* groups (Figure  
219 S5-S7).

220 In combination with our IYCF-by-PCoA effect modification models (see previous section), these  
221 findings indicate that infant microbiota species maturation characterized by a shift away from a  
222 microbiome dominated by *B. longum* (i.e. greater PCoA axis 1 score) was associated with a reduction in  
223 the probability of stunting at age 18mo in infants randomized to IYCF (Table 2). In contrast, species  
224 composition associated with mother-infant FUT2+/FUT3- phenotype (i.e. greater PCoA axis 2 score),  
225 which was characterized by higher *B. longum* abundance, showed evidence of reduced impact of IYCF on  
226 stunting (Table 2).

227

228 *Bifidobacterium longum* relative abundance modifies the effect of the IYCF intervention on stunting at  
229 18mo

230 To determine if differences in the relative abundances of specific microbiome species that  
231 characterized the constrained PCoA axes were also associated with significant modification of IYCF on  
232 stunting or LAZ at 18mo, we fitted multivariable regression models that included IYCF-by-species relative  
233 abundance interaction terms and prespecified covariates as described in the previous sections. These  
234 models were restricted to 53 infants who had a fecal specimen collected at the 6mo follow-up visit  
235 when IYCF started and used their covariate values at that visit (Figure S2). We fitted a separate model  
236 for each microbiome species of interest, defined as those strongly associated with PCoA axis 1 to 4  
237 scores (i.e. loadings > 0.5 or < -0.5). Infants randomized to IYCF who had greater relative abundance of  
238 *B. longum* when the intervention started were more likely to be stunted at age 18mo compared to  
239 infants with lower relative abundance of *B. longum* (differences-in-differences 50.0% [95%CI:  
240 26.0%,74.0%], adjusted  $p < 0.001$ ) (Table 3). No other species-level interactions with IYCF on stunting  
241 were identified (Table 3). Infants randomized to IYCF with greater *B. longum* relative abundance also  
242 had smaller LAZ at 18mo compared to infants with lower *B. longum* abundance; however, this  
243 association was not statistically significant after FDR-adjustment (differences-in-differences -0.88[95%CI:  
244 -1.45,-0.31], adjusted  $p = 0.074$ ) (Table S7). Overall, our findings indicate that greater relative abundance  
245 of *B. longum* in the infant gut microbiome at initiation of the IYCF intervention was associated with less  
246 efficacy of the IYCF intervention to reduce stunting at age 18mo.

247  
248 *Infants randomized to IYCF in the mother only FUT2+/FUT3- group or with lower B. longum relative*  
249 *abundance were spared from more severe growth faltering*

250 To investigate whether these reductions in IYCF efficacy were due to differences in the degree or  
251 timing of growth faltering, we plotted (i) LAZ growth trajectories and (ii) LAZ velocities (sd/mo) from 6-

252 18mo of age, by both IYCF arm and paired mother-infant FUT2+/FUT3- phenotype. Infants randomized  
253 to IYCF in the *mother only* group had a less steep decline in LAZ trajectories on average compared to  
254 infants in the *mother only* group randomized to no IYCF (Figure 1). In addition, although all groups of  
255 infants had negative 6-18mo LAZ velocities on average, infants in the *mother only* group who were  
256 randomized to IYCF had higher LAZ velocity (-0.02 sd/mo, 95%CI[-0.05,0.00]) compared to those in the  
257 no IYCF group (-0.08 sd/mo, 95%CI[-0.11,-0.05]) (Figure 1). Importantly, infants in the *mother only* group  
258 also benefitted more from the IYCF intervention in our interaction models (Table 1).

259 We repeated these exploratory analyses to compare LAZ trajectories and LAZ velocities by both IYCF  
260 arm and *B. longum* at the 6mo visit stratified above or below the relative abundance median. Infants  
261 randomized to IYCF who were above the median relative abundance of *B. longum* had declining growth  
262 trajectories on average, while infants below the median did not (Figure 2). Furthermore, the mean 6-  
263 18mo LAZ velocity was negative in both *B. longum* groups, but trended toward being higher in the group  
264 with relative abundance below (-0.02 sd/mo, 95%CI[-0.07,0.03]) compared to above (-0.08 sd/mo  
265 95%CI[-0.12,-0.03]) the median; however, the 95% confidence intervals overlapped. In contrast, among  
266 infants randomized to no IYCF, both those with a relative abundance above and those with a relative  
267 abundance below the median at the 6mo visit had declining growth trajectories (Figure 2) with similar  
268 average negative LAZ velocities (Figure 2).

269 Overall, these results indicate that the differences in IYCF efficacy by mother-infant FUT2+/FUT3-  
270 phenotype and *B. longum* relative abundance can be explained by differences in LAZ velocity. Infants in  
271 the *mother only* FUT2+/FUT3- group and infants with lower *B. longum* relative abundance at 6mo were  
272 spared from more severe LAZ declines, which contributed to a lower probability of stunting at 18mo,  
273 even when the differences in velocity were not statistically significant.

274



275 *Bifidobacterium longum* strains most similar to subspecies *infantis* dominate the early infant gut

276 *microbiome*

277 Next, we aimed to identify whether infants carried different strains of *B. longum* using a pangenome  
278 approach. We used PanPhlan3.0<sup>52</sup> to generate UniProt gene family profiles of dominant *B. longum*  
279 strains from 218 infant gut metagenomes, generated from 136 infant, with sufficient coverage of *B.*  
280 *longum* (Figure S2). To assess similarities between SHINE *B. longum* strains and previously characterized  
281 subspecies, we also included UniProt gene family profiles produced by PanPhlan for 118 reference  
282 strains. We performed PCoA using Jaccard dissimilarities calculated from these gene family presence or  
283 absence profiles. Three clusters of *B. longum* strains were identifiable by visualization of ordination plots  
284 (Figure 3 and S8). We, therefore, performed hierarchical clustering of these Jaccard dissimilarities to  
285 delineate three distinct strain clusters and place each strain into the most appropriate cluster (Figure  
286 S8). Subspecies *infantis* reference strains predominantly grouped with the largest cluster (hereafter  
287 called the *infantis* cluster) and included 15 *infantis* reference strains and 255 SHINE strains (Figure 3).  
288 Subspecies *longum* reference strains predominantly grouped with the second largest cluster (*longum*  
289 cluster), including 29 *longum*, 3 *infantis*, 64 *unclassified* subspecies strains and 14 SHINE strains. The  
290 remaining cluster included two subspecies *suis*, one subspecies *longum*, 4 *unclassified* subspecies  
291 reference strains and 15 SHINE strains (*suis* cluster) (Figure 3 and Figure S8).

292

293 *Infant gut microbiome maturation undergoes a transition in which Bifidobacterium longum* strains most  
294 *similar to subspecies infantis* become less prevalent

295 To investigate predictors of *B. longum* relative abundance in infants over time, we fitted a  
296 longitudinal multivariable zero-inflated mixed-effects model, using 225 specimens from 87 infants with  
297 prespecified covariate data. Covariates included infant age at specimen collection, sex, EBF at 3mo,  
298 minimum infant dietary diversity at specimen collection, and mother-infant FUT2+/FUT3- phenotypes

299 (Figure S2). Infant age and mother-infant FUT2+/FUT3- phenotype were significant predictors of *B.*  
300 *longum* relative abundance. Each one month increase in infant age was associated with a 0.91-fold  
301 decrease (95%CI:0.90,0.92,  $p < 0.001$ ) in *B. longum*, and the *mother only* FUT2+/FUT3- group had the  
302 lowest relative abundance of *B. longum* throughout follow-up (Figure S11) with a 0.71-fold decrease in  
303 relative abundance (95%CI:0.59,0.87,  $p = 0.001$ ) relative to the *both* group (Table S9).

304 Also, to determine predictors of *B. longum* strain cluster detection in infants over time, we fitted  
305 multivariable longitudinal logistic regression models using 133 specimens from 70 infants with  
306 PanPhlan3.0 output and prespecified covariate data (Figure S2). We fitted a separate model for each  
307 strain to estimate its probability of detection. Results were consistent with predictors of *B. longum*  
308 relative abundance. Each one month increase in infant age was associated with a 0.85-fold decreased  
309 odds (95%CI:0.75,0.96,  $p = 0.008$ ) of the *infantis* cluster (Table S10). At the same time, the *suis* and  
310 *longum* clusters increased with age (Table S10 & Figure S12). Female infants had 8.35-fold increased  
311 odds of the *infantis* cluster (95%CI:3.17,21.97,  $p < 0.001$ ); and the *infant only* FUT2+/FUT3- group, which  
312 had the highest probability of the *infantis* cluster throughout follow-up (Figure S13A), had a 4.66-fold  
313 increased odds (95%CI:1.05,20.71,  $p = 0.043$ ) of the *infantis* cluster (Table S10). In contrast, the *mother*  
314 *only* FUT2+/FUT3- group had low probability of carrying an *infantis* cluster strain (Figure S13A & Table  
315 S10) and the highest probability of carrying a *suis* cluster strain (Figure S13C).

316 In summary, *B. longum* decreased with infant age and was lowest among infants in the *mother only*  
317 FUT2+/FUT3- group. The *infantis* cluster, which included the dominant *B. longum* strains, also decreased  
318 with infant age. Furthermore, *infantis* cluster strains were most likely to be detected in the *infant only*  
319 group, and were less likely to be detected in the *mother only* group, among whom *suis* cluster strains  
320 were more likely to be detected. Infant age and mother-infant FUT2+/FUT3- phenotype were important  
321 determinants of both *B. longum* relative abundance and strain carriage.

322

323 *Bifidobacterium longum* strains most similar to subspecies *infantis* were characterized by greater  
324 capacity for HMO degradation, uptake, siderophore and antimicrobial biosynthesis

325 To identify differences in metabolic potential between *B. longum* strain clusters, we used two-sided  
326 Fisher's Exact tests to compare UniProt gene family presence between clusters. We restricted these  
327 analyses to the 284 SHINE *Bifidobacterium* pangenomes to make inferences about differences in  
328 metabolic potential between SHINE strains. We then performed overrepresentation analyses<sup>53</sup> of  
329 differentially frequent gene families by one-sided Fisher's Exact test to determine whether they were  
330 more likely to be involved in specific GO biological processes<sup>54</sup>, or to function as specific carbohydrate-  
331 active enzymes (CAZymes)<sup>55</sup> or transporters<sup>56</sup>. Gene families that were more common in the *infantis*  
332 cluster were more likely to be involved in HMO degradation, and included genes that function as  
333 CAZyme Glycoside Hydrolase Family 20 (GH20) ( $\beta$ -N-acetylglucosaminidases,  $\beta$ -N-  
334 acetylgalactosaminidase,  $\beta$ -6-SO<sub>3</sub>-N-acetylglucosaminidases, and lacto-N-biosidases), GH29  
335 (fucosidases), GH95 (fucosidases), and GH33 (sialidases) (Figure 4A, Table S8). Conversely, gene families  
336 that were more common in the other clusters were more likely to be involved in degradation of plant-  
337 derived polysaccharides, including genes that function as GH42 ( $\beta$ -galactosidases), GH51 (L-  
338 arabinofuranosidases) and GH127 ( $\beta$ -L-arabinofuranosidase) CAZymes (Figure 4A, Table S8). Similarly,  
339 gene families that were more common in the *infantis* cluster were more likely to function as  
340 transporters involved in oligosaccharide uptake (TCID 3.A.1.1.59), while those that were less common in  
341 the *infantis* cluster were more likely to be involved in uptake of fructose and other sugars (TCID  
342 3.A.1.2.23) (Figure 4A, Table S8). Other differences between strain clusters included greater carriage of  
343 gene families among *infantis* cluster strains that are involved in riboflavin biosynthesis, signal  
344 transduction, amino acid catabolism and uptake.

345 We also identified differences between strain clusters in the frequency of 115 MetaCyc<sup>57</sup> pathways  
346 identified using MinPath<sup>58</sup> (Figure S10). Pathways that were more common in the *infantis* cluster were

347 more likely to be involved in generation of precursor metabolites and energy, and secondary metabolite  
348 biosynthesis (which predominantly included pathways for biosynthesis of siderophores and  
349 antimicrobials) (Figure 4B, Table S8). Conversely, the *infantis* cluster was less likely to include pathways  
350 involved in glycan metabolism and polymeric compound degradation (e.g. pectin, xylan, and  
351 arabinogalactan degradation pathways), and in fatty acid and lipid biosynthesis (Figure 4B, Table S8).

352 Overall, infant gut microbiomes were dominated by *B. longum* strains that were most similar to  
353 subspecies *infantis* in their UniProt gene family profiles. The primary distinction of *B. longum* strains in  
354 the *infantis* cluster was greater capacity for HMO degradation and uptake of oligosaccharides than  
355 plant-derived polysaccharides. However, strains in the *infantis* cluster also had greater capacity for  
356 siderophore and antimicrobial production, and displayed differences in their capacity for riboflavin, fatty  
357 acid, and lipid metabolism.

358

## 359 Discussion

360 In this study of HIV-unexposed infants enrolled in the SHINE trial in rural Zimbabwe, we tested the  
361 hypothesis that mother-infant FUT2/FUT3 phenotype and infant gut microbiome modify the effect of an  
362 intervention containing small-quantity lipid based nutrient supplements, on infant stunting and LAZ at  
363 18mo of age. Our goal was to define mechanisms that explain the rather modest effects of SQ-LNS on  
364 linear growth, reasoning that maternal-infant HBGA phenotypes might be important given their  
365 combined role in shaping the early-life microbiome. We found the following features are associated with  
366 greater reduction in stunting at 18mo by IYCF: (i) discordance in mother-infant FUT2+/FUT3- phenotype,  
367 where the mother has the phenotype but the infant does not; (ii) changes in microbiome species  
368 composition that reflected a shift from a *B. longum*-dominant microbiome to a microbiome with less *B.*  
369 *longum* and a greater abundance of species characteristic of older infants; and (iii) decreased *B. longum*  
370 abundance that was associated with paired mother-infant FUT+/FUT3- status. These findings suggest

371 that a persistently “younger” microbiome, characterized by a high abundance of *B. longum* and carriage  
372 of *B. longum* strains best suited to HMO metabolism, at the point when complementary foods are  
373 introduced into the infant diet, may modify the effects of an intervention that includes SQ-LNS on infant  
374 stunting.

375 The *mother only* FUT2+/FUT3- group showed evidence of a greater reduction in stunting following  
376 receipt of one year of the IYCF intervention. Mother-infant FUT2+/FUT3- phenotype was also a  
377 significant predictor of *B. longum*, whereby relative abundance was lower throughout follow-up in the  
378 *mother only* group. Active maternal FUT2/FUT3 genes are key determinants of milk oligosaccharide  
379 composition<sup>31–33</sup>. Human milk specimens form distinct groups based on maternal FUT2<sup>59</sup> and FUT3  
380 phenotype<sup>31,33</sup> by principal component analyses of oligosaccharide composition. In particular,  
381 FUT2+/FUT3- mothers are a subset of FUT2+ women who form an HMO cluster that is distinct from  
382 mothers with other phenotypes, including FUT2+ mothers who are also FUT3+<sup>31,33</sup>. Differences in HMO  
383 composition influence growth and activity of Bifidobacterium populations in the infant gut<sup>28,59</sup>. Host  
384 FUT2 status may also affect infant gut microbiome composition<sup>36–40</sup>. Gut Bifidobacterium<sup>39</sup>,  
385 Bacteroides<sup>36,38</sup>, Faecalibacterium<sup>40</sup> and Roseburia<sup>40</sup> are differentially abundant in FUT2+ compared to  
386 FUT2- individuals. However, reported differences in microbiome composition by FUT2/FUT3 status have  
387 been inconsistent, potentially due to variability in age, dietary patterns, host health, sampled gut  
388 sections and methodology between studies<sup>60,614</sup>, and studies predominantly included adults. However,  
389 CAZymes found in *B. longum* species that function in HMO degradation (GH29 and GH95) have also been  
390 found to function in host intestinal glycan degradation in infants<sup>62</sup>. The evidence, therefore, suggests  
391 that the FUT2/FUT3 phenotypes of mother and infant, together, can elicit a strong prebiotic selective  
392 pressure, driven by maternal milk and infant glycan composition<sup>28</sup> that influences Bifidobacteria and  
393 broader gut microbiota composition in infants.

394 In contrast to our finding that mother-infant FUT2+/FUT3- phenotype predicted the presence of *B.*  
395 *longum* subspecies *infantis* cluster strains, a prior study reported that maternal or infant FUT2 or FUT3  
396 status did not predict the abundance of subspecies *infantis* or *longum* in children<sup>63</sup>. However, we  
397 included infant age as a covariate in our models, while the prior study did not<sup>63</sup>. In addition, to  
398 accommodate the fact that FUT2 and FUT3 work in concert biologically to produce different HBGAs and  
399 HMOs (Figure S1), we defined combined FUT2 and FUT3 phenotypes. Another smaller study found  
400 infants born to FUT2+/FUT3- mothers had lower bifidobacterial operational taxonomic unit diversity  
401 compared to other infants<sup>39</sup>. This study provides additional evidence that maternal FUT2+/FUT3-  
402 phenotype is associated with bifidobacterial taxon composition in the infant gut. Furthermore, we  
403 considered paired maternal and infant phenotypes<sup>63</sup>. More research is needed to clarify the roles of  
404 mother-infant FUT2/FUT3, maternal HMOs and the infant glyco biome as drivers of infant gut  
405 microbiome composition and development.

406 In our PCoA model, infant microbiome species maturation predominantly reflected decreased  
407 abundance of *B. longum* and increased abundance of *P. copri*, *F. prausnitzii*, *D. longicatena*, and *D.*  
408 *formicigenerans*. These species were also important predictors of infant age in a microbiome-age model  
409 previously developed from this same cohort<sup>64</sup>. Age-discriminatory taxa in the same genera were also  
410 identified in previously reported microbiome-age models<sup>14</sup>. Delayed gut microbiota-age has been  
411 reported in children with severe acute malnutrition (SAM), while improvements in microbiota-age and  
412 relative abundance of age-discriminatory taxa have been correlated with better growth<sup>14</sup>. Our analyses  
413 complement this literature with evidence that infant gut microbiome species maturation increased the  
414 effect of the IYCF intervention on stunting at 18mo, while greater relative abundance of *B. longum*, an  
415 age-discriminatory taxon which is associated with younger age, reduced the effect. This suggests that  
416 delayed maturation of the gut microbiome at the point when complementary foods are introduced and  
417 IYCF is initiated, may impair IYCF-induced effects on growth.

418 Infant age was the strongest determinant of *B. longum* relative abundance over time. This is  
419 consistent with previous reports<sup>65</sup>. In breastfed infants, Bifidobacteria are the most abundant gut  
420 bacteria<sup>65,66</sup>. Human breast milk is rich in oligosaccharides, which Bifidobacteria preferentially utilize<sup>67</sup>.  
421 At introduction of solid foods, a wider variety of nutrients and reduced availability of HMOs correspond  
422 to a decrease in Bifidobacterium,<sup>68</sup> greater bacterial diversity and evenness, and development of a more  
423 adult-like composition by 2–3 years of age<sup>11,69–71</sup>.

424 Utilization of HMOs by Bifidobacterium varies between species and strains<sup>72–78</sup>. We identified three  
425 clusters of dominant *B. longum* strains that also varied by infant age and mother-infant FUT2+/FUT3-  
426 phenotype. The cluster of strains with pangenomes most closely resembling subspecies *infantis* had the  
427 highest prevalence in early infancy. However, by age 18mo there was a marked decrease in detection of  
428 *infantis* cluster strains and a corresponding increase in detection of strains with pangenomes most  
429 similar to subspecies *suis*, which had the highest prevalence at 18mo. Strains most similar to subspecies  
430 *longum* increased more slowly. This finding is consistent with a recent study that also reported a pattern  
431 of succession among three distinct gut *B. longum* clades from birth to 24mo of age. Subspecies *infantis*  
432 was dominant in early infancy but peaked at age 6mo and decreased considerably thereafter. While a  
433 transitional clade that included strains most similar to subspecies *suis* and *suillum* showed a  
434 corresponding increase in abundance that peaked by 18mo, and subspecies *longum* expanded from  
435 15mo-24mo of age<sup>79</sup>. In that report, the transitional *suis/suillum* clade harbored functional capacity to  
436 degrade both HMOs and dietary polysaccharides, suggesting it may be an adaptation of the infant gut  
437 microbiome to a period when breastfeeding may co-occur with introduction of complementary foods<sup>79</sup>.  
438 We add to this work by showing that differences between mother and infant in FUT2+/FUT3- phenotype  
439 may also play a role in driving this transition, whereby, throughout follow-up, the *mother only*  
440 FUT2+/FUT3- group had a low prevalence of the *infantis* cluster and the highest prevalence of the *suis*  
441 cluster; while the *infantis* cluster was most prevalent in the *infant only* group.

442 *B. longum* subspecies *infantis* are particularly well adapted for HMO utilization<sup>80,81</sup>. *B. longum*  
443 subspecies *longum*, on the other hand, do not grow as well on HMO, and are more specialized for  
444 utilization of diet-derived polysaccharides<sup>82</sup>. In our analyses, UniProt gene families that were more  
445 frequent in the *infantis* cluster were more likely to be involved in HMO degradation and uptake. Two of  
446 CAZyme families more likely to be carried by the *infantis* cluster (GH29<sup>83</sup> and GH33<sup>74</sup>) were previously  
447 reported as more prevalent in subspecies *infantis* strains. In contrast, UniProt gene families that were  
448 less frequent in the *infantis* cluster were more likely to be involved in uptake of fructose and other  
449 simple sugars, including the sugar transporter 3.A.1.2.23, which was previously described in a different  
450 *B. longum* subspecies<sup>84</sup>. Furthermore, strains in the *suis* and *longum* clusters were more likely to carry  
451 UniProt gene families involved in such MetaCyc pathways as pectin, xylan, and arabinogalactan  
452 degradation. UniProt gene families found more frequently in *infantis* cluster strains were also more  
453 likely to be involved in siderophore and antimicrobial biosynthesis. Heavy metals such as iron and zinc  
454 are essential minerals for nearly all bacteria and their mammalian hosts. Strategies utilized by bacteria  
455 to acquire heavy metals include siderophore biosynthesis. Siderophores are low molecular weight iron-  
456 chelating compounds that are synthesized by bacteria to scavenge iron and other essential metals such  
457 as zinc under nutrient-restricted conditions<sup>85</sup>. For example, Bifidobacterium species isolated from iron-  
458 deficient children efficiently sequester iron via siderophore production<sup>86</sup>. Siderophores may provide a  
459 competitive advantage to Bifidobacteria<sup>87</sup>, which along with antimicrobial biosynthesis<sup>88</sup>, may also help  
460 protect the infant gut from enteric pathogens that require essential metals for colonization. However,  
461 essential metals such as iron and zinc are key components in SQ-LNS formulations<sup>89-91</sup>, and produce  
462 improvements in linear growth and reductions in stunting risk<sup>92,936</sup>. While siderophore activity varies  
463 considerably between Bifidobacterium species and strains, no research to date has investigated  
464 sequestration of essential metals by subspecies *infantis* strains commonly found in resource-limited  
465 settings. Overall, our analyses suggest that greater abundance of *B. longum*, at the time when IYCF is



466 started, characterized by a predominance of strains with carriage of gene families which confer greater  
467 capacity for HMO utilization and siderophore biosynthesis, is associated with lower impact to reduce  
468 stunting at 18mo. These suggest potential mechanisms by which a “younger” microbiome may constrain  
469 the beneficial effects of an SQ-LNS intervention on infant stunting. However, more research is required  
470 to fully elucidate the biological mechanisms and downstream pathways to stunting that could be  
471 involved.

472 Our results are in contrast to a previous RCT that investigated infant microbiome composition as a  
473 modifier of SQ-LNS impact on infant growth in Malawi<sup>48</sup>. However, in the primary analyses of that RCT,  
474 there was no effect of SQ-LNS on linear infant growth<sup>94</sup>. Furthermore, SQ-LNS was provided to both  
475 mothers during pregnancy and infants starting at 6mo postpartum, active control interventions (iron-  
476 folate or multiple micronutrient supplements) were provided to mothers<sup>48,94</sup>, and 16S rRNA gene  
477 amplification and sequencing were used to characterize the microbiota which can affect both taxon  
478 detection (including *Bifidobacterium*) and study results<sup>95</sup>. A second RCT reported evidence for effect  
479 modification of iron supplementation on growth by maternal FUT2 status, where infants of FUT2-  
480 mothers randomized to iron supplementation showed greater declines in LAZ than infants of FUT2+  
481 mothers<sup>96</sup>. In addition, a third, recent RCT found that suppression of *B. longum* by amoxicillin allowed  
482 the gut microbiota of children with SAM to better adapt to a solid-food diet by reducing the abundance  
483 of taxa specialized for breast milk utilization, resulting in improved anthropometric indicators of infant  
484 nutritional status<sup>97</sup>. However, it is essential to note that *B. longum* subspecies *infantis* is a critical early  
485 infant gut bacteria with important benefits for infant health, including protection from enteric  
486 pathogens<sup>98</sup>, immune system development<sup>99</sup>, and reducing asthma risk<sup>100</sup>. *B. longum* subspecies *infantis*  
487 also improved ponderal growth when administered to infants ~4mo of age with SAM in two RCTs<sup>101,102</sup>.  
488 However, the effects on LAZ were not statistically significant. Our work complements this literature. Our  
489 findings suggest that a shift away from a “less mature” microbiome, characterized by a high abundance

490 of *B. longum* and carriage of strains that are better suited to HMO metabolism, may be critical to  
491 support efficacy of nutrient supplements that start with the introduction of complementary feeding; and  
492 we identify maternal drivers of early infant *B. longum* abundance and strain carriage which, if further  
493 elucidated, may be employed to shape the infant microbiome into a more favorable composition at this  
494 critical time in infancy.

495       There are some limitations of this work. First, from our cohort of 1169 HIV-unexposed infants, we  
496 had microbiome data on 172 infants. However, infants included in our analyses were comparable to  
497 infants who excluded (Table S6). Also, mother-infant FUT2+/FUT3- phenotype, which was an important  
498 determinant of *B. longum* abundance and strain cluster detection, modified the impact of IYCF on  
499 stunting in the larger sample of 792 infants without measured microbiome data in a way that was  
500 consistent with our microbiome results. That said, our small sample size may have limited power to  
501 detect effect modification by other taxa that are indicative of a “more mature” post-weaning  
502 microbiome. Our analyses were not able to investigate effect modification by actual microbial metabolic  
503 activity, maternal HMO composition or infant gut glyco biome, which would require multi-omics  
504 approaches such as metatranscriptomics and metabolomics. Finally, it is possible that the delay in  
505 microbiome maturation we characterized may reflect some reverse causality, where sick or non-thriving  
506 children are put to the breast more with higher relative breastmilk intake. However, this behavior would  
507 need to systematically occur less often in the subset of mothers and their infants who were discordant  
508 for FUT2+/FUT3- that we describe to fully explain our results, thus we think this explanation is unlikely.

509       In conclusion, we present analyses of moderators of IYCF impact on infant stunting at 18mo in an  
510 RCT of IYCF using SQ-LNS in rural Zimbabwe. We report that (i) infant microbiome species maturation,  
511 characterized by a shift from *B. longum* dominance, particularly *B. longum* strains that are most similar  
512 to the proficient HMO utilizer subspecies *infantis*, was associated with increased IYCF reduction of  
513 stunting risk at age 18mo; (ii) discordance in mother-infant FUT2+/FUT3- phenotype, where the mother

514 had the phenotype but the infant did not, was associated with increased IYCF reduction of stunting risk;  
515 and (iii) reduction in *B. longum* relative abundance was also determined by mother-infant FUT2+/FUT3-  
516 phenotype. Future work should investigate how differences between maternal HMOs and infant gut  
517 glycans determine gut Bifidobacterium species and strain composition, and investigate how to tailor  
518 interventions at the introduction of complementary feeding to balance infant nutritional needs with  
519 age-related microbiome composition and function to prevent stunting.

520

## 521 **Figure legends**

### 522 **Figure 1. Infant growth trajectories and growth velocities vary by IYCF arm and mother-infant** 523 **FUT2+/FUT3- phenotype.**

524 (A) LAZ by infant age from 1-18mo (n=792), stratified by IYCF arm (light grey, no IYCF; dark grey, IYCF)  
525 and mother-infant FUT2+/FUT3- phenotype (*both, none, infant only or mother only*). Lines illustrate  
526 average trajectories. Shaded areas are 95% confidence bands. Infants randomized to IYCF in the *mother*  
527 *only* group had a less steep decline in LAZ trajectories on average compared to infants randomized to no  
528 IYCF.

529 (B) Violin plots of LAZ velocity from 6-18mo of age, stratified by IYCF arm (light grey, no IYCF; dark grey,  
530 IYCF) and mother-infant FUT2+/FUT3- phenotype (*both, none, infant only or mother only*). Open circles  
531 with error bars in the center of each panel indicate mean LAZ velocity and 95% CIs. All groups of infants  
532 had negative LAZ velocities on average, but infants in the *mother only* group who were randomized to  
533 IYCF had higher LAZ velocity on average, contributing to a less steep decline in LAZ over time and a  
534 smaller proportion of infants stunted at 18mo.

535

### 536 **Figure 2. Infant growth trajectories and growth velocities vary by IYCF arm and infant gut** 537 ***Bifidobacterium longum* relative abundance.**

538 (A) LAZ by infant age from 1-18mo (n=53), stratified by IYCF arm and *Bifidobacterium longum* relative  
539 abundance (light grey,  $\leq$ median relative abundance; dark grey,  $>$ median relative abundance). Thin lines  
540 illustrate individual trajectories. Thick lines show average trajectories. Infants randomized to IYCF who  
541 were above the median relative abundance had a declining growth trajectory on average, while infants  
542 below the median did not.

543 (B) Violin plots of LAZ velocity from 6-18mo of age, stratified by IYCF arm (light grey, no IYCF; dark grey,  
544 IYCF) and mother-infant FUT2+/FUT3- phenotype (*both, none, infant only* or *mother only*). Open circles  
545 with error bars indicate mean LAZ velocity and 95% CIs. All groups of infants had negative LAZ velocities  
546 on average. However, LAZ velocity trended toward being higher in the group with relative abundance  
547 below the median. The 95% confidence intervals overlap, but the higher LAZ velocity contributed to a  
548 less steep decline in LAZ over time and a smaller proportion of stunted infants at 18mo.

549

550 **Figure 3. *Bifidobacterium longum* strains most similar to subspecies *infantis* dominate the early infant**  
551 **gut microbiome.** Ordination plots of PCoA with Jaccard dissimilarities calculated using the pangenome  
552 profiles of dominant *Bifidobacterium longum* strains in fecal specimens (N=284) generated using  
553 PanPhlan3.0. Three clusters of *B. longum* strains were identifiable. Individual strains are indicated by  
554 small circles. Those in the same cluster are enclosed by a large ellipse and are differentiated by both the  
555 color of the ellipse and the border color of the small circle (blue, *infantis*; dark green, *longum*; red, *suis*).  
556 Filled small circles indicate reference strains (light blue, *infantis*; pink, *suis*, light green, *longum*; grey,  
557 *unclassified*). Open small circles indicate SHINE strains. Subspecies *infantis* reference strains  
558 predominantly grouped with the largest cluster (blue ellipse, *infantis* cluster). Subspecies *longum*  
559 reference strains predominantly grouped with the second largest cluster (dark green ellipse, *longum*  
560 cluster). The remaining cluster (red ellipse, *suis* cluster) grouped with subspecies *suis* and *longum*.

561

562 **Figure 4. SHINE infant *Bifidobacterium longum infantis* cluster strains are better adapted for human**  
563 **milk oligosaccharide utilization and protection against pathogens than *suis* and *longum* cluster strains.**

564 (A) Heatmap of UniProt gene family presence in SHINE infant *Bifidobacterium longum* strains (N=284).  
565 UniProt gene family presence is indicated in grey. The horizontal bar at the top indicates strain cluster  
566 (blue, *infantis*; dark green, *longum*; red, *suis*). Vertical bars from left to right indicate: UniProt gene  
567 families that differed in prevalence between the *infantis* and *longum* cluster by two-sided Fisher's Exact  
568 test after FDR correction (red); UniProt gene families that differed in prevalence between the *infantis*  
569 and *suis* cluster by two-sided Fisher's Exact test after FDR correction (red); Biological Process GO groups;  
570 CAZymes; and Transporter class. Only gene families with evidence of overrepresentation in a Biological  
571 Process, CAZyme or Transporter class by one-sided Fisher's Exact Test are presented.

572 (B) Heatmap of MetaCyc pathway presence in SHINE infant *Bifidobacterium longum* strains (N=284).  
573 MetaCyc pathway presence is indicated in grey. The horizontal bar at the top indicates strain cluster  
574 (blue, *infantis*; dark green, *longum*; red, *suis*). Vertical bars from left to right indicate: MetaCyc pathways  
575 that differed in prevalence between the *infantis* and *longum* cluster by two-sided Fisher's Exact test  
576 after FDR correction (red); MetaCyc pathways that differed in prevalence between the *infantis* and *suis*  
577 cluster by two-sided Fisher's Exact test after FDR correction (red); MetaCyc pathway type. Only  
578 pathways with evidence of overrepresentation in a pathway type by one-sided Fisher's Exact Test are  
579 presented.

580

## 581 **Methods**

### 582 *Study design and participants*

583 The Sanitation Hygiene Infant Nutrition Efficacy (SHINE) trial was a 2x2 factorial cluster-randomized  
584 trial that enrolled 5280 pregnant women at a median age of 12.5 weeks gestation between November  
585 2012 and March 2015 to test the impact of improved household water quality, sanitation, and hygiene

586 (WASH) and improved infant and young child feeding (IYCF) via provision of SQ-LNS to the infant from  
587 age 6mo-18mo, on linear growth and anemia at age 18mo. A detailed description of the SHINE trial  
588 design and methods has been published<sup>51,103</sup>.

589 Briefly, research nurses made home visits twice during pregnancy and at infant ages 1, 3, 6, 12, and  
590 18 months. At baseline, maternal education and age, household wealth<sup>104</sup>, existing water and sanitation  
591 services, and household food security<sup>105</sup> were assessed, and mothers were tested for HIV via a rapid  
592 testing algorithm. Infant birth date, weight, and delivery details were transcribed from health facility  
593 records. Gestational age at delivery was calculated from the date of the mother's last menstrual period  
594 ascertained at baseline. Infant weight, length, and mid-upper arm circumference were measured at  
595 every postnatal visit. Nurses were standardized against a gold-standard anthropometrist every 6  
596 months, with retraining provided to those who failed to meet predefined criteria.

597 Part-way through the trial (from mid-2014 onwards) mother-infant pairs were invited to join a  
598 substudy to collect additional biological specimens. Women were informed about the substudy at their  
599 32-week gestation visit and those with live births were enrolled at the 1-month postnatal visit, or as  
600 soon as possible thereafter<sup>106,107</sup>.

601

#### 602 *Specimen collection and processing*

603 Mothers collected fecal specimens prior to the research nurse visit. Fecal specimens were placed in  
604 a cold box and transported to the field laboratory, where they were stored at -80°C until transfer to the  
605 central laboratory in Harare for long-term archiving at -80°C, with generator back-up. Fecal specimens  
606 were transferred via private courier on dry ice from Harare, Zimbabwe to Vancouver, British Columbia  
607 for metagenomic analyses.

608 The Qiagen DNeasy PowerSoil Kit was used to extract total DNA from 200mg of feces, according to  
609 manufacturer's instructions. Paired-end libraries were constructed using the Illumina TruSeq kit and

610 using New England Biosystem TruSeq compatible library preparation reagents. Libraries were sequenced  
611 at the British Columbia Genome Sciences Centre using the Illumina HiSeq 2500 platform. Forty-eight  
612 libraries were pooled and included per sequencing lane. Negative controls were included to capture  
613 microbial contamination in the DNA extraction and library preparation steps.

614 The analyses presented here utilize data and specimens from HIV-uninfected mothers and their  
615 infants enrolled in the specimen collection substudy. The fecal microbiome was characterized in 354  
616 specimens collected from 172 HIV-unexposed infants from 1 to 18mo of age. A mean(sd) of 2.0(1.0)  
617 samples were analyzed per child. Infants included in these analyses largely resembled the population of  
618 live-born infants from the wider SHINE trial who were not included in these analyses (Table S6).  
619 However, infants in the current analyses had slightly older mothers and longer gestational ages, and  
620 fewer were born during the hungry season, but more were in a household that met the minimum  
621 dietary diversity score (Table S6). Overall, the majority were born by vaginal delivery (91.6%) in an  
622 institution (91.5%) and were exclusively breastfed (83.2% at 3 months). The prevalence of stunting was  
623 26.9% at 18mo in this sub-study (Table S6).

624

### 625 *Bioinformatics*

626 Sequenced reads were trimmed of adapters and filtered to remove low-quality, short (<60 base-  
627 pairs), and duplicate reads, as well as those of human, other animal or plant origin using KneadData with  
628 default settings. Overall, 354 unique whole metagenome sequencing datasets were used from fecal  
629 specimens collected from 1mo to 18mo from 172 infants with available mother and infant FUT2 and  
630 FUT3 phenotypes (Figure S2). On average,  $10.8 \pm 3.7$  million paired end quality-filtered reads were  
631 generated per sample. Assessment of negative controls and technical variation have been previously  
632 reported<sup>64</sup>. Species composition was determined by mapping reads to clade-specific markers using  
633 MetaPhlAn3, while functional gene and metabolic pathway composition was determined using

634 HUMAnN3 against the UniRef90 database, both with default settings<sup>52</sup>. Bacterial species and pathway  
635 abundance estimates were normalized to relative abundances. UniProt gene family profiles were  
636 generated for dominant *B. longum* strains in fecal metagenomes with sufficient coverage for  
637 pangenome analysis using PanPhlan3<sup>52</sup>. To facilitate interpretation of UniProt gene family profiles, the  
638 minimum set of biological pathways sufficient to explain the gene families identified in each strain was  
639 determined using MinPath with default settings<sup>58</sup> and the MetaCyc database<sup>57</sup>.

640

#### 641 *Assessment of FUT2 and FUT3 status*

642 Saliva samples were collected by oral swab from mothers and infants. Available saliva from any  
643 follow-up visit was selected to assess FUT2 and FUT3 status. Secretor versus non-secretor (FUT2) and  
644 Lewis-positive versus Lewis-null (FUT3) status were ascertained for infants and their mothers using a  
645 previously reported phenotyping assay<sup>108</sup>. We defined FUT2 and FUT3 phenotype combinations as  
646 Lewis-positive non-secretors (FUT2-/FUT3+), Lewis-positive secretors (FUT+/FUT3+), or Lewis-null  
647 secretors (FUT2+/FUT3-) (Table S11) according to the histo-blood group antigen synthesis pathways  
648 defined in Figure S1. Paired mother-infant phenotype concordance or discordance was defined as  
649 presented in Table S1.

650 Of 1,169 mother-infant pairs, 999 (85.4%) mothers and 1104 (94.4%) infants were tested. Of these,  
651 FUT2 or FUT3 status could be determined in 889 (76.0%) and 999 (85.4%) mothers and infants,  
652 respectively (Table S11). Of those whose FUT2 or FUT3 status could be ascertained, secretors were the  
653 most frequent FUT2 phenotype (88.1% and 85.6% in mothers and infants respectively), while Lewis-  
654 positive was the most frequent FUT3 phenotype (76.8% and 74.9% in mothers and infants, respectively)  
655 (Table S11). Most mothers and infants were Lewis-positive secretors (60.5% and 64.9%, respectively),  
656 followed by FUT2+/FUT3- (25.1% and 23.2%, respectively), and Lewis-positive non-secretors (14.4% and  
657 11.9%, respectively) (Table S1).



658

659 *Statistical analyses*

660 Infant characteristics that explain species  $\beta$ -diversity were evaluated using constrained principal  
661 coordinates analysis (PCoA) of Bray-Curtis dissimilarities (*capscale*)<sup>109</sup>. Characteristics of interest  
662 included factors that are known to be correlated with microbiome composition (infant age, sex, EBF at  
663 3mo, dietary diversity, maternal and infant FUT2 and FUT3 phenotype). Statistical significance was  
664 tested by permutational analysis of variance using distance matrices with 1000 permutations  
665 (*adonis2*)<sup>110</sup>. We then developed a final multivariable constrained PCoA model that included covariates  
666 which explained a significant fraction ( $p < 0.05$ ) of the variance in microbiome composition (infant age at  
667 specimen collection), as well as mother-infant FUT2+/FUT3- discordance given our *a priori* hypothesis  
668 that FUT2 and FUT3 phenotypes are important determinants of infant microbiome composition and our  
669 finding that mother-infant FUT2+/FUT3- discordance was an important modifier of IYCF efficacy to  
670 reduce stunting at 18mo. Constrained PCoA axis scores in the final multivariable model represented  
671 changes in microbiome composition (species turnover) along gradients defined by each infant  
672 characteristic included in the full model.

673 Since the IYCF intervention was started at the 6mo follow-up visit, we assessed interaction between  
674 randomization to IYCF and mother-infant FUT2+/FUT3- discordance or microbiome composition using  
675 data from the 6mo visit as covariates. The primary outcome was stunting at 18mo and LAZ at 18mo was  
676 a secondary outcome. We fitted separate models for stunting and LAZ at 18mo. Interaction was  
677 assessed on the additive risk difference scale, which is most appropriate for statistical estimation of  
678 synergistic biological effects<sup>111</sup>. We used generalized linear models (*glm*) with a Gaussian distribution, an  
679 identity link, sandwich standard errors (*sandwich*)<sup>112</sup> and an IYCF-by-mother-infant FUT2+/FUT3-  
680 phenotype interaction term. We repeated these analyses using IYCF-by-PCoA axis score interaction  
681 terms, where PCoA axis scores were derived from the final multivariable constrained PCoA model. One

682 model was fitted per constrained PCoA axis. For species that were strongly associated with PCoA axis  
683 scores (loadings > 0.5 or < -0.5), analyses were repeated to assess IYCF-by-species interactions. We fitted  
684 a separate model for each species of interest. Models also included IYCF, infant sex, mother-infant  
685 FUT2+/FUT3- discordance, infant age at specimen collection, an indicator of whether infants met the  
686 minimum dietary diversity score at specimen collection, and LAZ at specimen collection. We did not  
687 include WASH arm because, in prior analyses, the SHINE WASH intervention did not affect stunting or  
688 LAZ at 18mo<sup>51</sup> nor infant gut microbiome composition<sup>64</sup>. P-values were adjusted for multiple hypothesis  
689 testing to preserve the false discovery rate<sup>113</sup>.

690

#### 691 *Identification and analysis of Bifidobacterium longum strain clusters*

692 *B. longum* strain profiles produced with PanPhlan3.0, which indicate whether UniProt gene families  
693 are present in a strain<sup>114</sup>, were converted to Jaccard dissimilarity matrices and visualized by PCoA to  
694 ascertain the existence of strain clusters (*capscale*). Three clusters were identified, and strain cluster  
695 membership was determined by hierarchical clustering of Jaccard dissimilarities and Ward's error sum of  
696 squares algorithm (*hclust*)<sup>115</sup>. Hierarchical clustering dendrograms were cut at a height to obtain three  
697 clusters.

698 Differences in UniProt gene family profiles between *B. longum* strain clusters were determined by  
699 two-sided Fisher's Exact test (*fisher.test*), with adjustment for multiple hypothesis testing to preserve  
700 the false discovery rate<sup>113</sup>, and were visualized using heatmaps (*heatmap3*). 3260 UniProt gene families  
701 were differentially present between strain clusters after FDR-adjustment. We performed  
702 overrepresentation analyses<sup>53</sup> using one-sided Fisher's Exact tests (*fisher.test*) to determine whether the  
703 differentially present gene families were more likely to function as particular CAZymes<sup>55</sup> or  
704 transporters<sup>56</sup>, or in specific GO biological processes<sup>54</sup>. These analyses were repeated using the  
705 biological pathways determined with MinPath<sup>58</sup>. 115 pathways were differentially present between

706 strain clusters after FDR-adjustment. We performed overrepresentation analyses of these pathways to  
707 determine whether they were more likely to have particular biological functions defined by MetaCyc  
708 pathway types.

709

#### 710 *Predictors of Bifidobacterium relative abundance and strain detection*

711 Predictors of *B. longum* relative abundance over time were assessed using mixed-effects zero-  
712 inflated beta regression estimated by restricted maximum likelihood (*gamlss*)<sup>116</sup>. The model included  
713 infant age at specimen collection, sex, EBF at 3mo, minimum infant dietary diversity at specimen  
714 collection, and mother-infant FUT2+/FUT3- discordance, with random intercepts (*re*) and a first order  
715 autocorrelation structure (*corCAR1*).

716 Predictors of *B. longum* strain cluster were assessed by logistic regression (*glm*) using an indicator of  
717 strain cluster presence as the dependent variable, with the same covariates, and sandwich standard  
718 errors. An individual model was fitted separately for each cluster. Bias corrected<sup>117</sup> logistic regression  
719 was used to facilitate stable parameter estimation due to separation resulting from the small sample  
720 size<sup>118</sup>.

721 All statistical analyses were conducted in R version 4.2.0. PCoA and adonis2 were performed using  
722 the *vegan* package<sup>119</sup>. Heatmaps were generated with *heatmap3*. Mixed-effects zero-inflated beta  
723 regression was performed using the *gamlss* package<sup>120</sup>. Bias corrected logistic regression models were  
724 fitted using the *brglm2* package. Sandwich standard errors were generated with the *sandwich* package.

725

#### 726 *Resource availability*

#### 727 **Lead contact**

728 Further information and requests for resources and reagents should be directed to and will be fulfilled  
729 by the lead contact, Ethan Gough ([egough1@jh.edu](mailto:egough1@jh.edu)).

730 **Materials availability**

731 This study did not generate new unique reagents.

732 **Data and code availability**

733 The raw metagenome sequencing data generated in this study have been deposited in the European  
734 Bioinformatics Database under accession code PRJEB51728. Final processed and annotated  
735 metagenome sequencing data files (taxa and pathways) are available at

736 <https://doi.org/10.5281/zenodo.7471082>. **Epidemiologic data files are available at** Code for statistical  
737 analyses are available from the corresponding author upon request.

738

739 **Supplemental Tables**

740 **Table S8. Overrepresentation of UniProt gene families and Metacyc pathways, which differ between**  
741 **strain clusters, by GO biological process, CAZyme or Transporter class or Metacyc pathway type.**

742

743 **Ethics approvals**

744 All SHINE mothers provided written informed consent. The Medical Research Council of Zimbabwe  
745 (MRCZ/A/1675), Johns Hopkins Bloomberg School of Public Health (JHU IRB # 4205.), and the University  
746 of British Columbia Ethics Board (H15-03074) approved the study protocol, including the microbiome  
747 analyses. The SHINE trial is registered at ClinicalTrials.gov (NCT01824940).

748

749 **Acknowledgments**

750 We thank all the mothers, babies, and their families who participated in the SHINE trial and all members  
751 of the SHINE trial team (all members listed here: <https://doi.org/10.1093/cid/civ844>). We particularly  
752 thank the leadership and staff of the Ministry of Health and Child Care in Chirumanzu and Shurugwi  
753 districts and Midlands Province (especially environmental health, nursing, and nutrition) for their roles

754 in operationalization of the study procedures, the Ministry of Local Government officials in each district  
755 who supported and facilitated field operations, Phillipa Rambanepasi and her team for proficient  
756 management of all the finances, Virginia Sauramba for management of compliance issues, and the  
757 programme officers at the Bill & Melinda Gates Foundation and the Department for International  
758 Development (UK Aid), who enthusiastically worked with us over a long period to make SHINE happen.  
759 Funding was from the Bill & Melinda Gates Foundation (OPP1021542 and OPP1143707; J.H.H. and  
760 A.J.P.), with a subcontract to the University of British Columbia (20R25498; A.R.M.). United Kingdom  
761 Department for International Development (DFID/UKAID; J.H.H. and A.J.P.). Wellcome Trust  
762 (093768/Z/10/Z, 108065/Z/15/Z, 206455/Z/17/Z, 203905/Z/16/Z and 210807/Z/18/Z; A.J.P., R.C.R. and  
763 C.E.). Swiss Agency for Development and Cooperation (J.H.H. and A.J.P.). US National Institutes of Health  
764 (2R01HD060338-06; J.H.H.). UNICEF (PCA-2017-0002; J.H.H. and A.J.P.). The Nutricia Research  
765 Foundation (2021-52; E.K.G.) The funders had no role in the design of the study and collection, analysis,  
766 and interpretation of data and in writing the manuscript.

767  
768 **Author contributions:** A.R.M., L.E.S., R.J.S., M.N.N.M., J.H.H. and A.J.P. conceptualized and designed the  
769 study. K.M., R.N., B.C., F.D.M., N.V.T., J.T., and B.M. collected data and biospecimens. H.M.G., I.B.,  
770 S.K.G., R.C.R., F.F. and L.C. processed fecal specimens. M.K. conducted laboratory analyses to ascertain  
771 FUT2 and FUT3 status. C.E., J.C. and E.K.G. developed the FUT2 and FUT3 analysis plan. E.K.G. developed  
772 and conducted the microbiome statistical analysis plan. T.J.E. and E.K.G. conducted bioinformatics.  
773 A.R.M. and E.K.G. analyzed and interpreted the data. E.K.G. wrote the original manuscript draft. All  
774 authors reviewed the manuscript. A.R.M., A.J.P. and J.H.H. supervised and verified the data.

775

776 **Declaration of interests:** T.J.E. was paid a scientific consulting fee in relation to the analysis of the data  
777 presented here by the Zvitambo Institute for Maternal and Child Health Research. All other authors  
778 declare no competing interests.

779

780

781

782

783

784

785

786

787

788

789

790

791

792

793

794

795

**Table 1. Multivariable regression model<sup>1</sup> to estimate modification of IYCF on stunting at 18mo by mother-infant Lewis-null secretor phenotype discordance among 792 infants in whom mother and infant FUT2 and FUT3 status was ascertained**

	<u>Main Effect</u>			<u>Difference-in-Differences for IYCF by FUT2 and FUT3 phenotype combination</u>		
	PD (95%CI)	p-value	Adjusted p-value <sup>2</sup>	PD (95%CI)	p-value	Adjusted p-value <sup>2</sup>
Both FUT2+/FUT3-	ref	ref	ref	ref	ref	
None FUT2+/FUT3-	0.13(0.01,0.25)	0.041	0.330	-0.21(-0.42,-0.01)	0.039	0.118
Infant only FUT2+/FUT3-	0.15(-0.03,0.33)	0.094	0.277	-0.21(-0.48,0.06)	0.127	0.191
Mom only FUT2+/FUT3-	0.29(0.14,0.44)	0.000	0.007	-0.33(-0.55,-0.10)	0.005	0.015
non-IYCF	ref	ref	ref			
IYCF	0.16(-0.02,0.35)	0.138	0.177			

<sup>1</sup>Covariates include season of birth, birthweight, infant sex, ever exclusive breastfeeding at 3mo, age at the 6mo visit, infant WHZ at the 6mo visit, and infant LAZ at the 6mo visit

<sup>2</sup>Adjusted for multiple hypothesis testing by the Benjamini-Hochberg method

PD, prevalence difference; 95%CI, 95% confidence interval; ref, referent

796

797

798

799

800

801

802

803

804

805

806

807

808

809

810  
811  
812  
813  
814

**Table 2. Multivariable regression models<sup>1</sup> to estimate modification of IYCF on stunting at 18mo by infant gut microbiome species turnover in 53 infants**

	PD(95%CI)	p-value	Adjusted p-value <sup>2</sup>
<b>PCoA Axis 1</b>		<u>n/N=17/53</u>	
<b>IYCF</b>	-0.51(-0.99,-0.12)	0.009	0.045
<b>PC1</b>	0.21(-0.99,0.45)	0.085	0.204
<b>PC1-by-IYCF<sup>3</sup></b>	-0.76(-0.99,-0.32)	0.001	0.003
<b>PCoA Axis 2</b>		<u>n/N=17/53</u>	
<b>IYCF</b>	-0.14(-0.99,0.12)	0.293	0.469
<b>PC2</b>	-0.06(-0.99,-0.01)	0.020	0.068
<b>PC2-by-IYCF<sup>3</sup></b>	0.14(0.07,0.21)	<0.001	0.001
<b>PCoA Axis 3</b>		<u>n/N=17/53</u>	
<b>IYCF</b>	0.09(-0.99,0.39)	0.543	0.686
<b>PC3</b>	0.04(-0.99,0.09)	0.156	0.340
<b>PC3-by-IYCF<sup>3</sup></b>	-0.08(-0.99,-0.02)	0.016	0.032
<b>PCoA Axis 4</b>		<u>n/N=17/53</u>	
<b>IYCF</b>	0.03(-0.99,0.31)	0.847	0.924
<b>PC4</b>	0.00(-0.99,0.06)	0.994	0.994
<b>PC4-by-IYCF<sup>3</sup></b>	0.03(-0.99,0.12)	0.438	0.501

<sup>1</sup>Covariates include birthweight, infant sex, age at the 6mo visit, infant LAZ at the 6mo visit, infant diet diversity score at the 6mo visit, and mother-infant Lewis-null secretor phenotype discordance coded as both, none, infant only or mother only

<sup>2</sup>Adjusted for multiple hypothesis testing by the Benjamini-Hochberg method

<sup>3</sup>Differences-in-differences

PD, prevalence difference; 95%CI, 95% confidence interval

815  
816  
817  
818  
819



820

821

**Table 3. Multivariable regression models<sup>1</sup> to estimate modification of IYCF on stunting at 18mo by infant gut microbiome species in 53 infants**

	PD(95%CI)	p-value	Adjusted p-value <sup>2</sup>
Bifidobacterium longum		<u>n/N=17/53</u>	
IYCF	-0.16(-0.43,0.10)	0.232	0.976
B.longum	-0.24(-0.43,-0.05)	0.014	0.068
B.longum-by-IYCF <sup>3</sup>	0.50(0.26,0.74)	<0.001	<0.001
Bifidobacterium pseudocatenulatum		<u>n/N=17/53</u>	
IYCF	-0.54(-1.02,-0.06)	0.029	0.304
B.pseudocatenulatum	1.82(0.48,3.15)	0.008	0.051
B.pseudocatenulatum-by-IYCF <sup>3</sup>	-2.00(-3.33,-0.68)	0.003	0.014
Escherichia coli		<u>n/N=17/53</u>	
IYCF	0.04(-0.25,0.33)	0.774	1.000
E.coli	0.01(-0.10,0.13)	0.823	0.859
E.coli-by-IYCF <sup>3</sup>	-0.07(-0.21,0.08)	0.362	0.592
Dorea longicatena		<u>n/N=17/53</u>	
IYCF	0.02(-0.27,0.31)	0.896	1.000
D.longicatena	-0.02(-0.13,0.09)	0.725	0.859
D.longicatena-by-IYCF <sup>3</sup>	0.03(-0.39,0.44)	0.898	0.898
Dorea formicigenerans		<u>n/N=17/53</u>	
IYCF	-0.18(-0.37,0.01)	0.062	0.324
D.formicigenerans	-0.18(-0.33,-0.03)	0.018	0.073
D.formicigenerans-by-IYCF <sup>3</sup>	-0.50(-1.00,-0.00)	0.048	0.145

<sup>1</sup>Covariates include birthweight, infant sex, age at the 6mo visit, infant LAZ at the 6mo visit, infant diet diversity score at the 6mo visit, and mother-infant Lewis-null secretor phenotype discordance coded as both, none, infant only or mother only

<sup>2</sup>Adjusted for multiple hypothesis testing by the Benjamini-Hochberg method

<sup>3</sup>Differences-in-differences

PD, prevalence difference; 95%CI, 95% confidence interval

822

823

824

825

826

827

828 **References**

- 829 1. United Nations Children’s Fund, World Health Organization, and The World Bank (2019). Levels  
830 and trends in child malnutrition: key findings of the 2019 Edition of the Joint Child Malnutrition  
831 Estimates – UNICEF Regions. (United Nations Children’s Fund (UNICEF), World Health Organization,  
832 International Bank for Reconstruction and Development/The World Bank).
- 833 2. Onis, M.D., Garza, C., Onyango, A.W., and Martorell, R. (2006). WHO child growth standards. *Acta*  
834 *Paediatrica* 95, 1–104.
- 835 3. Benjamin-Chung, J., Mertens, A., Colford, J.M., Hubbard, A.E., van der Laan, M.J., Coyle, J.,  
836 Sofrygin, O., Cai, W., Nguyen, A., Pokpongkiat, N.N., et al. (2023). Early-childhood linear growth  
837 faltering in low- and middle-income countries. *Nature* 621, 550–557.
- 838 4. Gough, E.K., Moodie, E.E.M., Prendergast, A.J., Ntozini, R., Moulton, L.H., Humphrey, J.H., Manges,  
839 A.R., Stephens, D.A., Moodie, E.E.M., Prendergast, A.J., et al. (2016). Linear growth trajectories in  
840 Zimbabwean infants. *American Journal of Clinical Nutrition* 104, 1616–1627.
- 841 5. Adair, L.S.L.S., Fall, C.H.D.D., Osmond, C., Stein, A.D.A.A.D., Martorell, R., Ramirez-Zea, M.,  
842 Sachdev, H.S., Dahly, D.L., Bas, I., Norris, S.A., et al. (2013). Associations of linear growth and  
843 relative weight gain during early life with adult health and human capital in countries of low and  
844 middle income: Findings from five birth cohort studies. *The Lancet* 382, 525–534.
- 845 6. Victora, C.G., Adair, L., Fall, C., Hallal, P.C., Martorell, R., Richter, L., and Sachdev, H.S. (2008).  
846 Maternal and child undernutrition: consequences for adult health and human capital. *Lancet* 371,  
847 340–357.
- 848 7. Vollmer, S., Harttgen, K., Subramanyam, M.A., Finlay, J., Klasen, S., and Subramanian, S.V. (2014).  
849 Association between economic growth and early childhood undernutrition: evidence from 121  
850 Demographic and Health Surveys from 36 low-income and middle-income countries. *The Lancet*  
851 *Global Health* 2, e225-234.
- 852 8. Dewey, K.G., Wessells, K.R., Arnold, C.D., Prado, E.L., Abbeddou, S., Adu-Afarwuah, S., Ali, H.,  
853 Arnold, B.F., Ashorn, P., Ashorn, U., et al. (2021). Characteristics that modify the effect of small-  
854 quantity lipid-based nutrient supplementation on child growth: an individual participant data  
855 meta-analysis of randomized controlled trials. *Am J Clin Nutr* 114, 15S-42S.
- 856 9. Dewey, K.G., Arnold, C.D., Wessells, K.R., Prado, E.L., Abbeddou, S., Adu-Afarwuah, S., Ali, H.,  
857 Arnold, B.F., Ashorn, P., Ashorn, U., et al. (2022). Preventive small-quantity lipid-based nutrient  
858 supplements reduce severe wasting and severe stunting among young children: an individual  
859 participant data meta-analysis of randomized controlled trials. *Am J Clin Nutr* 116, 1314–1333.

- 860 10. Ruel, M.T., Alderman, H., and Maternal Child Nutrition Study Group (2013). Nutrition-sensitive  
861 interventions and programmes: how can they help to accelerate progress in improving maternal  
862 and child nutrition? *Lancet* 382, 536–551.
- 863 11. Arrieta, M.-C., Stiemsma, L.T., Amenyogbe, N., Brown, E.M., and Finlay, B. (2014). The intestinal  
864 microbiome in early life: health and disease. *Frontiers in Immunology* 5, 427.
- 865 12. Jones, H.J., Bourke, C.D., Swann, J.R., and Robertson, R.C. (2023). Malnourished Microbes: Host–  
866 Microbiome Interactions in Child Undernutrition. *Annual Review of Nutrition* 43, 327–353.
- 867 13. Robertson, R.C., Manges, A.R., Finlay, B.B., and Prendergast, A.J. (2019). The Human Microbiome  
868 and Child Growth - First 1000 Days and Beyond. *Trends Microbiol* 27, 131–147.
- 869 14. Subramanian, S., Huq, S., Yatsunenkov, T., Haque, R., Mahfuz, M., Alam, M.A., Benezra, A.,  
870 DeStefano, J., Meier, M.F., Muegge, B.D., et al. (2014). Persistent gut microbiota immaturity in  
871 malnourished Bangladeshi children. *Nature* 510, 417–421.
- 872 15. Zhao, G., Vatanen, T., Droit, L., Park, A., Kostic, A.D., Poon, T.W., Vlamakis, H., Siljander, H.,  
873 Härkönen, T., Hämäläinen, A.M., et al. (2017). Intestinal virome changes precede autoimmunity in  
874 type I diabetes-susceptible children. *Proceedings of the National Academy of Sciences of the*  
875 *United States of America* 114, E6166–E6175. 10.1073/pnas.1706359114.
- 876 16. Ho, N.T., Li, F., Lee-Sarwar, K.A., Tun, H.M., Brown, B.P., Pannaraj, P.S., Bender, J.M., Azad, M.B.,  
877 Thompson, A.L., Weiss, S.T., et al. (2018). Meta-analysis of effects of exclusive breastfeeding on  
878 infant gut microbiota across populations. *Nature Communications* 9, 4169. 10.1038/s41467-018-  
879 06473-x.
- 880 17. Reyes, A., Blanton, L.V., Cao, S., Zhao, G., Manary, M., Trehan, I., Smith, M.I., Wang, D., Virgin,  
881 H.W., Rohwer, F., et al. (2015). Gut DNA viromes of Malawian twins discordant for severe acute  
882 malnutrition. *Proceedings of the National Academy of Sciences of the United States of America*  
883 112, 11941–11946. 10.1073/pnas.1514285112.
- 884 18. Gough, E.K., Stephens, D.A., Moodie, E.M., Prendergast, A.J., Stoltzfus, R.J., Humphrey, J.H., and  
885 Manges, A.R. (2016). Linear growth faltering in infants is associated with *Acidaminococcus* sp. and  
886 community-level changes in the gut microbiota. *Microbiome* 3, 24.
- 887 19. Ghosh, T.S., Gupta, S.S., Bhattacharya, T., Yadav, D., Barik, A., Chowdhury, A., Das, B., Mande, S.S.,  
888 and Nair, G.B. (2014). Gut Microbiomes of Indian Children of Varying Nutritional Status. *PLoS ONE*  
889 9, e95547.
- 890 20. Gupta, S.S., Mohammed, M.H., Ghosh, T.S., Kanungo, S., Nair, G.B., and Mande, S.S. (2011).  
891 Metagenome of the gut of a malnourished child. *Gut Pathog* 3, 7.
- 892 21. Huey, S.L., Jiang, L., Fedarko, M.W., McDonald, D., Martino, C., Ali, F., Russell, D.G., Udipi, S.A.,  
893 Thorat, A., Thakker, V., et al. (2020). Nutrition and the Gut Microbiota in 10- to 18-Month-Old  
894 Children Living in Urban Slums of Mumbai, India. *mSphere* 5, e00731-20.

- 895 22. Digitale, J., Sié, A., Coulibaly, B., Ouermi, L., Dah, C., Tapsoba, C., Bärnighausen, T., Lebas, E., Arzika,  
896 A.M., Glymour, M.M., et al. (2020). Gut Bacterial Diversity and Growth among Preschool Children  
897 in Burkina Faso. *Am J Trop Med Hyg* *103*, 2568–2573.
- 898 23. Collard, J.-M., Andrianonimiadana, L., Habib, A., Rakotondrainipiana, M., Andriantsalama, P.,  
899 Randriamparany, R., Rabenandrasana, M. a. N., Weill, F.-X., Sauvonnet, N., Rendremanana, R.V., et  
900 al. (2022). High prevalence of small intestine bacteria overgrowth and asymptomatic carriage of  
901 enteric pathogens in stunted children in Antananarivo, Madagascar. *PLoS Negl Trop Dis* *16*,  
902 e0009849.
- 903 24. Kamng'ona, A.W., Young, R., Arnold, C.D., Kortekangas, E., Patson, N., Jorgensen, J.M., Prado, E.L.,  
904 Chaima, D., Malamba, C., Ashorn, U., et al. (2019). The association of gut microbiota characteristics  
905 in Malawian infants with growth and inflammation. *Scientific Reports* *9*.
- 906 25. Perin, J., Burrowes, V., Almeida, M., Ahmed, S., Haque, R., Parvin, T., Biswas, S., Azmi, I.J., Bhuyian,  
907 S.I., Talukder, K.A., et al. (2020). A Retrospective Case-Control Study of the Relationship between  
908 the Gut Microbiota, Enteropathy, and Child Growth. *The American journal of tropical medicine and*  
909 *hygiene*.
- 910 26. Brown, E.M., Wlodarska, M., Willing, B. p, Vonaesch, P., Han, J., Reynolds, L.A., Arriet, M.-C., Uhrig,  
911 M., Scholz, R., Partida, O., et al. (2015). Diet and specific microbial exposure trigger features of  
912 environmental enteropathy in a novel murine model. *Nature Communications* *6*, 7806.
- 913 27. Kau, A.L., Planer, J.D., Liu, J., Rao, S., Yatsunencko, T., Trehan, I., Manary, M.J., Liu, T.-C.,  
914 Stappenbeck, T.S., Maleta, K.M., et al. (2015). Functional characterization of IgA-targeted bacterial  
915 taxa from undernourished Malawian children that produce diet-dependent enteropathy. *Science*  
916 *Translational Medicine* *7*, 276ra24-276ra24.
- 917 28. Salli, K., Hirvonen, J., Siitonen, J., Ahonen, I., Anglenius, H., and Maukonen, J. (2021). Selective  
918 Utilization of the Human Milk Oligosaccharides 2'-Fucosyllactose, 3-Fucosyllactose, and  
919 Difucosyllactose by Various Probiotic and Pathogenic Bacteria. *Journal of Agricultural and Food*  
920 *Chemistry* *69*.
- 921 29. Davis, J.C.C., Totten, S.M., Huang, J.O., Nagshbandi, S., Kirmiz, N., Garrido, D.A., Lewis, Z.T., Wu,  
922 L.D., Smilowitz, J.T., German, J.B., et al. (2016). Identification of Oligosaccharides in Feces of  
923 Breast-fed Infants and Their Correlation with the Gut Microbial Community\*. *Molecular & Cellular*  
924 *Proteomics* *15*, 2987–3002.
- 925 30. Charbonneau, M.R., O'Donnell, D., Blanton, L.V., Totten, S.M., Davis, J.C.C., Barratt, M.J., Cheng, J.,  
926 Guruge, J., Talcott, M., Bain, J.R., et al. (2016). Sialylated Milk Oligosaccharides Promote  
927 Microbiota-Dependent Growth in Models of Infant Undernutrition. *Cell* *164*, 859–871.
- 928 31. Mank, M., Hauner, H., Heck, A.J.R., and Stahl, B. (2020). Targeted LC-ESI-MS2 characterization of  
929 human milk oligosaccharide diversity at 6 to 16 weeks post-partum reveals clear staging effects  
930 and distinctive milk groups. *Anal Bioanal Chem* *412*, 6887–6907.
- 931 32. Castanys-Muñoz, E., Martin, M.J., and Prieto, P.A. (2013). 2'-fucosyllactose: an abundant,  
932 genetically determined soluble glycan present in human milk. *Nutr Rev* *71*, 773–789.

- 933 33. Blank, D., Dotz, V., Geyer, R., and Kunz, C. (2012). Human milk oligosaccharides and Lewis blood  
934 group: individual high-throughput sample profiling to enhance conclusions from functional studies.  
935 *Adv Nutr* 3, 440S-9S.
- 936 34. Schneider, M., Al-Shareffi, E., and Haltiwanger, R.S. (2017). Biological functions of fucose in  
937 mammals. *Glycobiology* 27, 601–618.
- 938 35. Cooling, L. (2015). Blood groups in infection and host susceptibility. *Clinical Microbiology Reviews*  
939 28.
- 940 36. Tong, M., McHardy, I., Ruegger, P., Goudarzi, M., Kashyap, P.C., Haritunians, T., Li, X., Graeber,  
941 T.G., Schwager, E., Huttenhower, C., et al. (2014). Reprogramming of gut microbiome energy  
942 metabolism by the FUT2 Crohn’s disease risk polymorphism. *ISME J* 8, 2193–2206.
- 943 37. Rausch, P., Rehman, A., Künzel, S., Häsler, R., Ott, S.J., Schreiber, S., Rosenstiel, P., Franke, A., and  
944 Baines, J.F. (2011). Colonic mucosa-associated microbiota is influenced by an interaction of crohn  
945 disease and FUT2 (Secretor) genotype. *Proceedings of the National Academy of Sciences of the*  
946 *United States of America* 108.
- 947 38. Gampa, A., Engen, P.A., Shobar, R., and Mutlu, E.A. (2017). Relationships between gastrointestinal  
948 microbiota and blood group antigens. *Physiol Genomics* 49, 473–483.
- 949 39. Wacklin, P., Mäkivuokko, H., Alakulppi, N., Nikkilä, J., Tenkanen, H., Råbinä, J., Partanen, J., Aranko,  
950 K., and Mättö, J. (2011). Secretor genotype (FUT2 gene) is strongly associated with the  
951 composition of bifidobacteria in the human intestine. *PLoS ONE* 6, e20113.
- 952 40. Rühlemann, M.C., Hermes, B.M., Bang, C., Doms, S., Moitinho-Silva, L., Thingholm, L.B., Frost, F.,  
953 Degenhardt, F., Wittig, M., Kässens, J., et al. (2021). Genome-wide association study in 8,956  
954 German individuals identifies influence of ABO histo-blood groups on gut microbiome. *Nat Genet*  
955 53, 147–155.
- 956 41. Christensen, L., Vuholm, S., Roager, H.M., Nielsen, D.S., Krych, L., Kristensen, M., Astrup, A., and  
957 Hjorth, M.F. (2019). Prevotella Abundance Predicts Weight Loss Success in Healthy, Overweight  
958 Adults Consuming a Whole-Grain Diet Ad Libitum: A Post Hoc Analysis of a 6-Wk Randomized  
959 Controlled Trial. *J Nutr* 149, 2174–2181.
- 960 42. Eriksen, A.K., Brunius, C., Mazidi, M., Hellström, P.M., Risérus, U., Iversen, K.N., Fristedt, R., Sun, L.,  
961 Huang, Y., Nørskov, N.P., et al. (2020). Effects of whole-grain wheat, rye, and lignan  
962 supplementation on cardiometabolic risk factors in men with metabolic syndrome: a randomized  
963 crossover trial. *Am J Clin Nutr* 111, 864–876. 10.1093/ajcn/nqaa026.
- 964 43. Shin, J.-H., Jung, S., Kim, S.-A., Kang, M.-S., Kim, M.-S., Joung, H., Hwang, G.-S., and Shin, D.-M.  
965 (2019). Differential Effects of Typical Korean Versus American-Style Diets on Gut Microbial  
966 Composition and Metabolic Profile in Healthy Overweight Koreans: A Randomized Crossover Trial.  
967 *Nutrients* 11, E2450.
- 968 44. Hjorth, M.F., Roager, H.M., Larsen, T.M., Poulsen, S.K., Licht, T.R., Bahl, M.I., Zohar, Y., and Astrup,  
969 A. (2018). Pre-treatment microbial Prevotella-to-Bacteroides ratio, determines body fat loss  
970 success during a 6-month randomized controlled diet intervention. *Int J Obes (Lond)* 42, 580–583.

- 971 45. Li, Y., Wang, D.D., Satija, A., Ivey, K.L., Li, J., Wilkinson, J.E., Li, R., Baden, M., Chan, A.T.,  
972 Huttenhower, C., et al. (2021). Plant-Based Diet Index and Metabolic Risk in Men: Exploring the  
973 Role of the Gut Microbiome. *J Nutr* *151*, 2780–2789.
- 974 46. Li, J., Li, Y., Ivey, K.L., Wang, D.D., Wilkinson, J.E., Franke, A., Lee, K.H., Chan, A., Huttenhower, C.,  
975 Hu, F.B., et al. (2022). Interplay between diet and gut microbiome, and circulating concentrations  
976 of trimethylamine N-oxide: findings from a longitudinal cohort of US men. *Gut* *71*, 724–733.
- 977 47. Wang, D.D., Nguyen, L.H., Li, Y., Yan, Y., Ma, W., Rinott, E., Ivey, K.L., Shai, I., Willett, W.C., Hu, F.B.,  
978 et al. (2021). The gut microbiome modulates the protective association between a Mediterranean  
979 diet and cardiometabolic disease risk. *Nat Med* *27*, 333–343.
- 980 48. Hughes, R.L., Arnold, C.D., Young, R.R., Ashorn, P., Maleta, K., Fan, Y.-M., Ashorn, U., Chaima, D.,  
981 Malamba-Banda, C., Kable, M.E., et al. (2020). Infant gut microbiota characteristics generally do  
982 not modify effects of lipid-based nutrient supplementation on growth or inflammation: secondary  
983 analysis of a randomized controlled trial in Malawi. *Sci Rep* *10*, 14861.
- 984 49. Smith, M.I., Yatsunencko, T., Manary, M.J., Trehan, I., Mkakosya, R., Cheng, J., Kau, A.L., Rich, S.S.,  
985 Concannon, P., Mychaleckyj, J.C., et al. (2013). Gut microbiomes of Malawian twin pairs discordant  
986 for Kwashiorkor. *Science* *339*, 548–554.
- 987 50. Schwarzer, M., Makki, K., Storelli, G., Machuca-Gayet, I., Srutkova, D., Hermanova, P., Martino,  
988 M.E., Balmand, S., Hudcovic, T., Heddi, A., et al. (2016). *Lactobacillus plantarum* strain maintains  
989 growth of infant mice during chronic undernutrition. *Science* *351*, 854–857.
- 990 51. Humphrey, J.H., Mbuya, M.N.N., Ntozini, R., Moulton, L.H., Stoltzfus, R.J., Tavengwa, N.V., Mutasa,  
991 K., Majo, F.D., Mutasa, B., Mangwadu, G., et al. (2019). Independent and combined effects of  
992 improved water, sanitation, and hygiene, and improved complementary feeding, on child stunting  
993 and anaemia in rural Zimbabwe: a cluster-randomised trial. *The Lancet Global Health* *7*, e132–  
994 e147.
- 995 52. Beghini, F., McIver, L.J., Blanco-Míguez, A., Dubois, L., Asnicar, F., Maharjan, S., Mailyan, A.,  
996 Manghi, P., Scholz, M., Thomas, A.M., et al. (2021). Integrating taxonomic, functional, and strain-  
997 level profiling of diverse microbial communities with bioBakery 3. *Elife* *10*, e65088.
- 998 53. Wieder, C., Frainay, C., Poupin, N., Rodriguez-Mier, P., Vinson, F., Cooke, J., Lai, R.P., Bundy, J.G.,  
999 Jourdan, F., and Ebbels, T. (2021). Pathway analysis in metabolomics: Recommendations for the  
1000 use of over-representation analysis. *PLoS Comput Biol* *17*, e1009105.
- 1001 54. The Gene Ontology Consortium, Aleksander, S.A., Balhoff, J., Carbon, S., Cherry, J.M., Drabkin, H.J.,  
1002 Ebert, D., Feuermann, M., Gaudet, P., Harris, N.L., et al. (2023). The Gene Ontology knowledgebase  
1003 in 2023. *Genetics* *224*, iyad031.
- 1004 55. Drula, E., Garron, M.-L., Dogan, S., Lombard, V., Henrissat, B., and Terrapon, N. (2022). The  
1005 carbohydrate-active enzyme database: functions and literature. *Nucleic Acids Res* *50*, D571–D577.
- 1006 56. Saier, M.H., Reddy, V.S., Moreno-Hagelsieb, G., Hendargo, K.J., Zhang, Y., Iddamsetty, V., Lam,  
1007 K.J.K., Tian, N., Russum, S., Wang, J., et al. (2021). The Transporter Classification Database (TCDB):  
1008 2021 update. *Nucleic Acids Res* *49*, D461–D467.

- 1009 57. Caspi, R., Billington, R., Fulcher, C.A., Keseler, I.M., Kothari, A., Krummenacker, M., Latendresse,  
1010 M., Midford, P.E., Ong, Q., Ong, W.K., et al. (2018). The MetaCyc database of metabolic pathways  
1011 and enzymes. *Nucleic Acids Research* *46*, D633–D639.
- 1012 58. Ye, Y., and Doak, T.G. (2009). A parsimony approach to biological pathway  
1013 reconstruction/inference for genomes and metagenomes. *PLoS Comput Biol* *5*, e1000465.
- 1014 59. Bazanella, M., Maier, T.V., Clavel, T., Lagkouvardos, I., Lucio, M., Maldonado-Gómez, M.X., Autran,  
1015 C., Walter, J., Bode, L., Schmitt-Kopplin, P., et al. (2017). Randomized controlled trial on the impact  
1016 of early-life intervention with bifidobacteria on the healthy infant fecal microbiota and  
1017 metabolome. *American Journal of Clinical Nutrition* *106*, 1274–1286.
- 1018 60. Davenport, E.R., Cusanovich, D.A., Michelini, K., Barreiro, L.B., Ober, C., and Gilad, Y. (2015).  
1019 Genome-wide association studies of the human gut microbiota. *PLoS ONE* *10*.  
1020 10.1371/journal.pone.0140301.
- 1021 61. Turpin, W., Bedrani, L., Espin-Garcia, O., Xu, W., Silverberg, M.S., Smith, M.I., Guttman, D.S.,  
1022 Griffiths, A., Moayyedi, P., Panaccione, R., et al. (2018). FUT2 genotype and secretory status are  
1023 not associated with fecal microbial composition and inferred function in healthy subjects. *Gut*  
1024 *Microbes* *9*.
- 1025 62. Bell, A., and Juge, N. (2021). Mucosal glycan degradation of the host by the gut microbiota.  
1026 *Glycobiology* *31*, 691–696.
- 1027 63. Colston, J.M., Taniuchi, M., Ahmed, T., Ferdousi, T., Kabir, F., Mduma, E., Nshama, R., Iqbal, N.T.,  
1028 Haque, R., Ahmed, T., et al. (2022). Intestinal Colonization With *Bifidobacterium longum*  
1029 Subspecies Is Associated With Length at Birth, Exclusive Breastfeeding, and Decreased Risk of  
1030 Enteric Virus Infections, but Not With Histo-Blood Group Antigens, Oral Vaccine Response or Later  
1031 Growth in Three Birth Cohorts. *Front Pediatr* *10*, 804798.
- 1032 64. Robertson, R.C., Edens, T.J., Carr, L., Mutasa, K., Gough, E.K., Evans, C., Geum, H.M., Baharmand, I.,  
1033 Gill, S.K., Ntozini, R., et al. (2023). The gut microbiome and early-life growth in a population with  
1034 high prevalence of stunting. *Nat Commun* *14*, 654.
- 1035 65. Stewart, C.J., Ajami, N.J., O'Brien, J.L., Hutchinson, D.S., Smith, D.P., Wong, M.C., Ross, M.C., Lloyd,  
1036 R.E., Doddapaneni, H.V., Metcalf, G.A., et al. (2018). Temporal development of the gut microbiome  
1037 in early childhood from the TEDDY study. *Nature* *562*, 583–588.
- 1038 66. Yatsunenko, T., Rey, F.E., Manary, M.J., Trehan, I., Dominguez-Bello, M.G., Contreras, M., Magris,  
1039 M., Hidalgo, G., Baldassano, R.N., Anokhin, A.P., et al. (2012). Human gut microbiome viewed  
1040 across age and geography. *Nature* *486*, 222–228.
- 1041 67. Marcobal, A., and Sonnenburg, J.L. (2012). Human milk oligosaccharide consumption by intestinal  
1042 microbiota: Human milk oligosaccharide consumption. *Clinical Microbiology and Infection* *18*, 12–  
1043 15.
- 1044 68. Bäckhed, F., Roswall, J., Peng, Y., Feng, Q., Jia, H., Kovatcheva-Datchary, P., Li, Y., Xia, Y., Xie, H.,  
1045 Zhong, H., et al. (2015). Dynamics and stabilization of the human gut microbiome during the first  
1046 year of life. *Cell Host and Microbe* *17*, 690–703. 10.1016/j.chom.2015.04.004.

- 1047 69. Collado, M.C., Cernada, M., Bäuerl, C., Vento, M., and Pérez-Martínez, G. (2012). Microbial ecology  
1048 and host-microbiota interactions during early life stages. *Gut Microbes* 3, 352–365.
- 1049 70. Matamoros, S., Gras-Leguen, C., Vacon, F.L., Potel, G., and Cochetiere, M.-F. de L. (2013).  
1050 Development of intestinal microbiota in infants and its impact on health. *Trends in Microbiology*  
1051 21, 167–173.
- 1052 71. Laursen, M.F. (2021). Gut Microbiota Development: Influence of Diet from Infancy to Toddlerhood.  
1053 *Annals of Nutrition and Metabolism*.
- 1054 72. Lewis, Z.T., Totten, S.M., Smilowitz, J.T., Popovic, M., Parker, E., Lemay, D.G., Van Tassell, M.L.,  
1055 Miller, M.J., Jin, Y.-S., German, J.B., et al. (2015). Maternal fucosyltransferase 2 status affects the  
1056 gut bifidobacterial communities of breastfed infants. *Microbiome* 3, 13.
- 1057 73. Ojima, M.N., Jiang, L., Arzamasov, A.A., Yoshida, K., Odamaki, T., Xiao, J., Nakajima, A., Kitaoka, M.,  
1058 Hirose, J., Urashima, T., et al. (2022). Priority effects shape the structure of infant-type  
1059 Bifidobacterium communities on human milk oligosaccharides. *ISME J* 16, 2265–2279.
- 1060 74. Li, M., Zhou, X., Stanton, C., Ross, R.P., Zhao, J., Zhang, H., Yang, B., and Chen, W. (2021).  
1061 Comparative Genomics Analyses Reveal the Differences between *B. longum* subsp. *infantis* and *B.*  
1062 *longum* subsp. *longum* in Carbohydrate Utilisation, CRISPR-Cas Systems and Bacteriocin Operons.  
1063 *Microorganisms* 9, 1713.
- 1064 75. Gotoh, A., Katoh, T., Sakanaka, M., Ling, Y., Yamada, C., Asakuma, S., Urashima, T., Tomabechi, Y.,  
1065 Katayama-Ikegami, A., Kurihara, S., et al. (2018). Sharing of human milk oligosaccharides  
1066 degradants within bifidobacterial communities in faecal cultures supplemented with  
1067 Bifidobacterium bifidum. *Scientific Reports* 8, 13958.
- 1068 76. Sakanaka, M., Gotoh, A., Yoshida, K., Odamaki, T., Koguchi, H., Xiao, J.-Z., Kitaoka, M., and  
1069 Katayama, T. (2019). Varied Pathways of Infant Gut-Associated Bifidobacterium to Assimilate  
1070 Human Milk Oligosaccharides: Prevalence of the Gene Set and Its Correlation with Bifidobacteria-  
1071 Rich Microbiota Formation. *Nutrients* 12, 71. 10.3390/nu12010071.
- 1072 77. Garrido, D., Ruiz-Moyano, S., Lemay, D.G., Sela, D.A., German, J.B., and Mills, D.A. (2015).  
1073 Comparative transcriptomics reveals key differences in the response to milk oligosaccharides of  
1074 infant gut-associated bifidobacteria. *Sci Rep* 5, 13517.
- 1075 78. Garrido, D., Ruiz-Moyano, S., Kirmiz, N., Davis, J.C., Totten, S.M., Lemay, D.G., Ugalde, J.A.,  
1076 German, J.B., Lebrilla, C.B., and Mills, D.A. (2016). A novel gene cluster allows preferential  
1077 utilization of fucosylated milk oligosaccharides in Bifidobacterium longum subsp. longum SC596.  
1078 *Sci Rep* 6, 35045.
- 1079 79. Vatanen, T., Ang, Q.Y., Siegwald, L., Sarker, S.A., Le Roy, C.I., Duboux, S., Delannoy-Bruno, O.,  
1080 Ngom-Bru, C., Boulangé, C.L., Stražar, M., et al. (2022). A distinct clade of Bifidobacterium longum  
1081 in the gut of Bangladeshi children thrives during weaning. *Cell* 185, 4280-4297.e12.
- 1082 80. Sela, D.A., Chapman, J., Adeuya, A., Kim, J.H., Chen, F., Whitehead, T.R., Lapidus, A., Rokhsar, D.S.,  
1083 Lebrilla, C.B., German, J.B., et al. (2008). The genome sequence of Bifidobacterium longum subsp.



- 1084 infantis reveals adaptations for milk utilization within the infant microbiome. Proceedings of the  
1085 National Academy of Sciences *105*, 18964–18969.
- 1086 81. Thomson, P., Medina, D.A., and Garrido, D. (2018). Human milk oligosaccharides and infant gut  
1087 bifidobacteria: Molecular strategies for their utilization. *Food Microbiology* *75*, 37–46.
- 1088 82. LoCascio, R.G., Desai, P., Sela, D.A., Weimer, B., and Mills, D.A. (2010). Broad conservation of milk  
1089 utilization genes in *Bifidobacterium longum* subsp. *infantis* as revealed by comparative genomic  
1090 hybridization. *Appl Environ Microbiol* *76*, 7373–7381.
- 1091 83. Fushinobu, S., and Abou Hachem, M. (2021). Structure and evolution of the bifidobacterial  
1092 carbohydrate metabolism proteins and enzymes. *Biochem Soc Trans* *49*, 563–578.
- 1093 84. Wei, X., Guo, Y., Shao, C., Sun, Z., Zhurina, D., Liu, D., Liu, W., Zou, D., Jiang, Z., Wang, X., et al.  
1094 (2012). Fructose Uptake in *Bifidobacterium longum* NCC2705 Is Mediated by an ATP-binding  
1095 Cassette Transporter. *Journal of Biological Chemistry* *287*, 357–367. 10.1074/jbc.M111.266213.
- 1096 85. Johnstone, T.C., and Nolan, E.M. (2015). Beyond Iron: Non-Classical Biological Functions of  
1097 Bacterial Siderophores. *Dalton Trans* *44*, 6320–6339.
- 1098 86. Vazquez-Gutierrez, P., Lacroix, C., Jaeggi, T., Zeder, C., Zimmerman, M.B., and Chassard, C. (2015).  
1099 *Bifidobacteria* strains isolated from stools of iron deficient infants can efficiently sequester iron.  
1100 *BMC Microbiol* *15*, 3.
- 1101 87. Vazquez-Gutierrez, P., de Wouters, T., Werder, J., Chassard, C., and Lacroix, C. (2016). High Iron-  
1102 Sequestering *Bifidobacteria* Inhibit Enteropathogen Growth and Adhesion to Intestinal Epithelial  
1103 Cells In vitro. *Front Microbiol* *7*, 1480.
- 1104 88. Gibson, G. r., and Wang, X. (1994). Regulatory effects of bifidobacteria on the growth of other  
1105 colonic bacteria. *Journal of Applied Bacteriology* *77*, 412–420.
- 1106 89. Arimond, M., Zeilani, M., Jungjohann, S., Brown, K.H., Ashorn, P., Allen, L.H., and Dewey, K.G.  
1107 (2015). Considerations in developing lipid-based nutrient supplements for prevention of  
1108 undernutrition: experience from the International Lipid-Based Nutrient Supplements (iLiNS)  
1109 Project. *Matern Child Nutr* *11*, 31–61.
- 1110 90. Beal, T., White, J.M., Arsenault, J.E., Okronipa, H., Hinnouho, G.-M., Murira, Z., Torlesse, H., and  
1111 Garg, A. (2021). Micronutrient gaps during the complementary feeding period in South Asia: A  
1112 Comprehensive Nutrient Gap Assessment. *Nutr Rev* *79*, 26–34.
- 1113 91. White, J.M., Beal, T., Arsenault, J.E., Okronipa, H., Hinnouho, G.-M., Chimanya, K., Matji, J., and  
1114 Garg, A. (2021). Micronutrient gaps during the complementary feeding period in 6 countries in  
1115 Eastern and Southern Africa: a Comprehensive Nutrient Gap Assessment. *Nutr Rev* *79*, 16–25.
- 1116 92. Park, J.J.H., Harari, O., Siden, E., Dron, L., Zannat, N.-E., Singer, J., Lester, R.T., Thorlund, K., and  
1117 Mills, E.J. (2020). Interventions to improve linear growth during complementary feeding period for  
1118 children aged 6-24 months living in low- and middle-income countries: a systematic review and  
1119 network meta-analysis [version 2; peer review: 3 approved]. *3*, 1660.

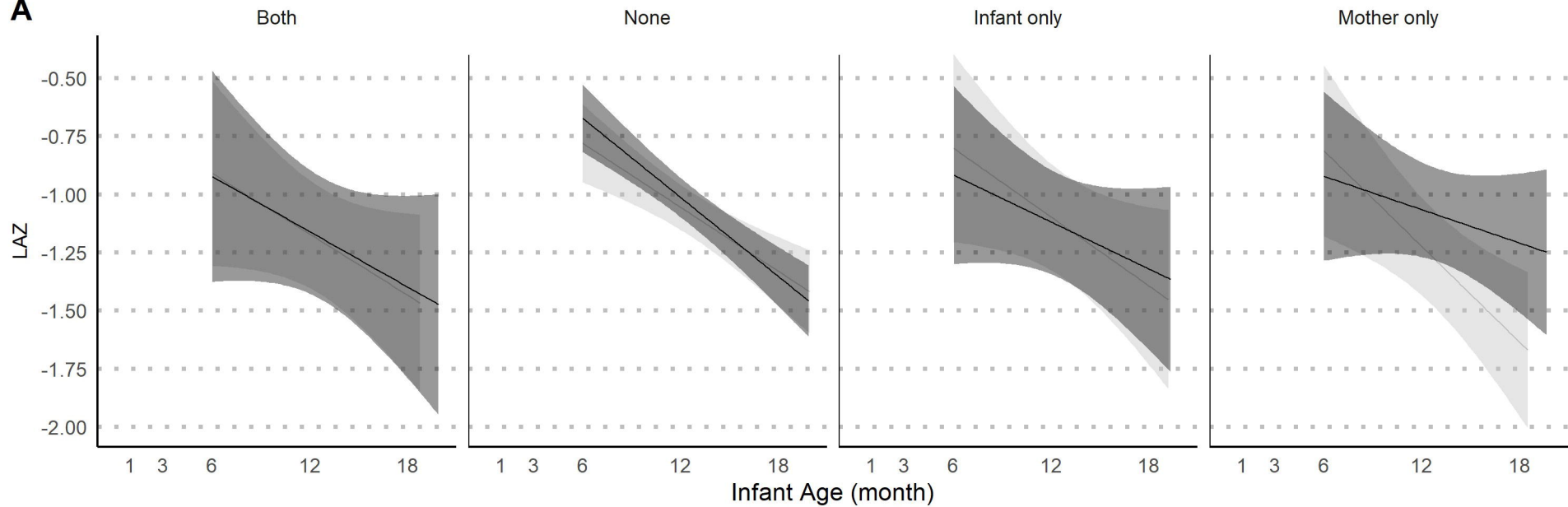
- 1120 93. Imdad, A., and Bhutta, Z.A. (2011). Effect of preventive zinc supplementation on linear growth in  
1121 children under 5 years of age in developing countries: a meta-analysis of studies for input to the  
1122 lives saved tool. *BMC Public Health* *11*, S22.
- 1123 94. Ashorn, P., Alho, L., Ashorn, U., Cheung, Y.B., Dewey, K.G., Gondwe, A., Harjunmaa, U., Lartey, A.,  
1124 Phiri, N., Phiri, T.E., et al. (2015). Supplementation of Maternal Diets during Pregnancy and for 6  
1125 Months Postpartum and Infant Diets Thereafter with Small-Quantity Lipid-Based Nutrient  
1126 Supplements Does Not Promote Child Growth by 18 Months of Age in Rural Malawi: A Randomized  
1127 Controlled Trial. *J Nutr* *145*, 1345–1353. 10.3945/jn.114.207225.
- 1128 95. Abellan-Schneyder, I., Matchado, M.S., Reitmeier, S., Sommer, A., Sewald, Z., Baumbach, J., List,  
1129 M., and Neuhaus, K. (2021). Primer, Pipelines, Parameters: Issues in 16S rRNA Gene Sequencing.  
1130 *mSphere* *6*, e01202-20.
- 1131 96. Paganini, D., Uyoga, M.A., Kortman, G.A.M., Boekhorst, J., Schneeberger, S., Karanja, S., Henet, T.,  
1132 and Zimmermann, M.B. (2019). Maternal Human Milk Oligosaccharide Profile Modulates the  
1133 Impact of an Intervention with Iron and Galacto-Oligosaccharides in Kenyan Infants. *Nutrients* *11*,  
1134 2596.
- 1135 97. Schwartz, D.J., Langdon, A., Sun, X., Langendorf, C., Berthé, F., Grais, R.F., Trehan, I., Isanaka, S.,  
1136 and Dantas, G. (2023). Effect of amoxicillin on the gut microbiome of children with severe acute  
1137 malnutrition in Madarounfa, Niger: a retrospective metagenomic analysis of a placebo-controlled  
1138 trial. *The Lancet Microbe* *4*, e931–e942.
- 1139 98. Ruiz, L., Flórez, A.B., Sánchez, B., Moreno-Muñoz, J.A., Rodríguez-Palmero, M., Jiménez, J., Gavilán,  
1140 C.G. de los R., Gueimonde, M., Ruas-Madiedo, P., and Margolles, A. (2020). *Bifidobacterium*  
1141 *longum* subsp. *infantis* CECT7210 (*B. infantis* IM-1®) Displays In Vitro Activity against Some  
1142 Intestinal Pathogens. *Nutrients* *12*, 3259.
- 1143 99. Henrick, B.M., Rodriguez, L., Lakshmikanth, T., Pou, C., Henckel, E., Arzoomand, A., Olin, A., Wang,  
1144 J., Mikes, J., Tan, Z., et al. (2021). *Bifidobacteria*-mediated immune system imprinting early in life.  
1145 *Cell* *184*, 3884-3898.e11.
- 1146 100. Dai, D.L.Y., Petersen, C., Hoskinson, C., Del Bel, K.L., Becker, A.B., Moraes, T.J., Mandhane, P.J.,  
1147 Finlay, B.B., Simons, E., Kozyrskyj, A.L., et al. (2023). Breastfeeding enrichment of *B. longum* subsp.  
1148 *infantis* mitigates the effect of antibiotics on the microbiota and childhood asthma risk. *Med* *4*, 92-  
1149 112.e5.
- 1150 101. Barratt, M.J., Nuzhat, S., Ahsan, K., Frese, S.A., Arzamasov, A.A., Sarker, S.A., Islam, M.M., Palit, P.,  
1151 Islam, M.R., Hibberd, M.C., et al. (2022). *Bifidobacterium infantis* treatment promotes weight gain  
1152 in Bangladeshi infants with severe acute malnutrition. *Sci Transl Med* *14*, eabk1107.
- 1153 102. Nuzhat, S., Hasan, S.M.T., Palit, P., Islam, M.R., Mahfuz, M., Islam, M.M., Alam, M.A., Flannery, R.L.,  
1154 Kyle, D.J., Sarker, S.A., et al. (2023). Effects of probiotic and synbiotic supplementation on ponderal  
1155 and linear growth in severely malnourished young infants in a randomized clinical trial. *Sci Rep* *13*,  
1156 1845.
- 1157 103. Humphrey, J.H., Jones, A.D., Manges, A., Mangwadu, G., Maluccio, J.A., Mbuya, M.N.N., Moulton,  
1158 L.H., Ntozini, R., Prendergast, A.J., Stoltzfus, R.J., et al. (2015). The sanitation hygiene infant

- 1159 nutrition efficacy (SHINE) Trial: Rationale, design, and methods. *Clinical Infectious Diseases* *61*,  
1160 S685-702.
- 1161 104. Chasekwa, B., Maluccio, J.A., Ntozini, R., Moulton, L.H., Wu, F., Smith, L.E., Matare, C.R., Stoltzfus,  
1162 R.J., Mbuya, M.N.N., Tielsch, J.M., et al. (2018). Measuring wealth in rural communities: Lessons  
1163 from the sanitation, hygiene, infant nutrition efficacy (SHINE) trial. *PLoS ONE* *13*, 1–19.
- 1164 105. Maxwell, D., Watkins, B., Wheeler, R., and Collins, G. (2003). The Coping Strategy Index: a tool for  
1165 rapid measurement of household food security and the impact of food aid programs in  
1166 humanitarian emergencies. (*CARE and WFP*).
- 1167 106. E.K, G., L.H, M., K, M., R, N., R.J, S., F.D, M., L.E, S., G, P., N, G., M, J., et al. (2020). Effects of  
1168 improved water, sanitation, and hygiene and improved complementary feeding on environmental  
1169 enteric dysfunction in children in rural Zimbabwe: A cluster-randomized controlled trial. *PLoS*  
1170 *Neglected Tropical Diseases* *14*, e0007963.
- 1171 107. Mutasa, K., Ntozini, R., Mbuya, M.N.N., Rukobo, S., Govha, M., Majo, F.D., Tavengwa, N., Smith,  
1172 L.E., Caulfield, L., Swann, J.R., et al. (2021). Biomarkers of environmental enteric dysfunction are  
1173 not consistently associated with linear growth velocity in rural Zimbabwean infants. *The American*  
1174 *journal of clinical nutrition* *113*.
- 1175 108. Colston, J.M., Francois, R., Pisanic, N., Yori, P.P., McCormick, B.J.J., Olortegui, M.P., Gazi, M.A.,  
1176 Svensen, E., Ahmed, M.M.M., Mduma, E., et al. (2019). Effects of Child and Maternal Histo-Blood  
1177 Group Antigen Status on Symptomatic and Asymptomatic Enteric Infections in Early Childhood.  
1178 *Journal of Infectious Diseases* *220*, 151–162.
- 1179 109. Legendre, P., and Anderson, M.J. (1999). Distance-Based Redundancy Analysis: Testing  
1180 Multispecies Responses in Multifactorial Ecological Experiments. *Ecological Monographs* *69*, 1–24.
- 1181 110. Anderson, M.J. (2001). A new method for non-parametric multivariate analysis of variance. *Austral*  
1182 *Ecology* *26*, 32–46.
- 1183 111. VanderWeele, T.J. (2012). Sample Size and Power Calculations for Additive Interactions. *Epidemiol*  
1184 *Methods* *1*, 159–188.
- 1185 112. Naimi, A.I., and Whitcomb, B.W. (2020). Estimating Risk Ratios and Risk Differences Using  
1186 Regression. *Am J Epidemiol* *189*, 508–510.
- 1187 113. Benjamini, Y., and Hochberg, Y. (1995). Controlling the False Discovery Rate: A Practical and  
1188 Powerful Approach to Multiple Testing. *Journal of the Royal Statistical Society. Series B*  
1189 *(Methodological)* *57*, 289–300.
- 1190 114. Scholz, M., Ward, D.V., Pasolli, E., Tolio, T., Zolfo, M., Asnicar, F., Truong, D.T., Tett, A., Morrow,  
1191 A.L., and Segata, N. (2016). Strain-level microbial epidemiology and population genomics from  
1192 shotgun metagenomics. *Nature Methods* *13*, 435–438.
- 1193 115. Murtagh, F., and Legendre, P. (2014). Ward’s Hierarchical Agglomerative Clustering Method:  
1194 Which Algorithms Implement Ward’s Criterion? *Journal of Classification* *31*, 274–295.

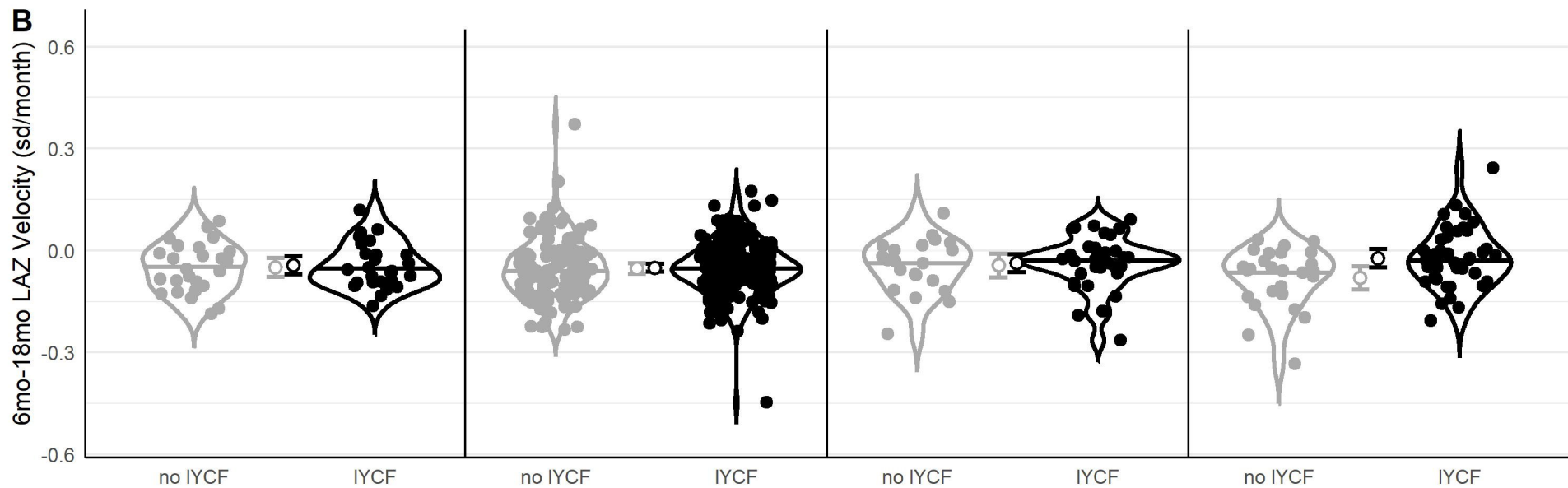
- 1195 116. Chen, E.Z., and Li, H. (2016). A two-part mixed-effects model for analyzing longitudinal microbiome  
1196 compositional data. In *Bioinformatics*, pp. 2611–2617. 10.1093/bioinformatics/btw308.
- 1197 117. Kosmidis, I., Kenne Pagui, E.C., and Sartori, N. (2020). Mean and median bias reduction in  
1198 generalized linear models. *Stat Comput* 30, 43–59.
- 1199 118. Mansournia, M.A., Geroldinger, A., Greenland, S., and Heinze, G. (2018). Separation in Logistic  
1200 Regression: Causes, Consequences, and Control. *Am J Epidemiol* 187, 864–870.
- 1201 119. Dixon, P. (2003). VEGAN, a package of R functions for community ecology. *Journal of Vegetation*  
1202 *Science* 14, 927–930.
- 1203 120. Stasinopoulos, D.M., and Rigby, R.A. (2007). Generalized additive models for location scale and  
1204 shape (GAMLSS) in R. *Journal of Statistical Software* 23, 1–46. 10.18637/jss.v023.i07.
- 1205
- 1206

no IYCF IYCF

**A**

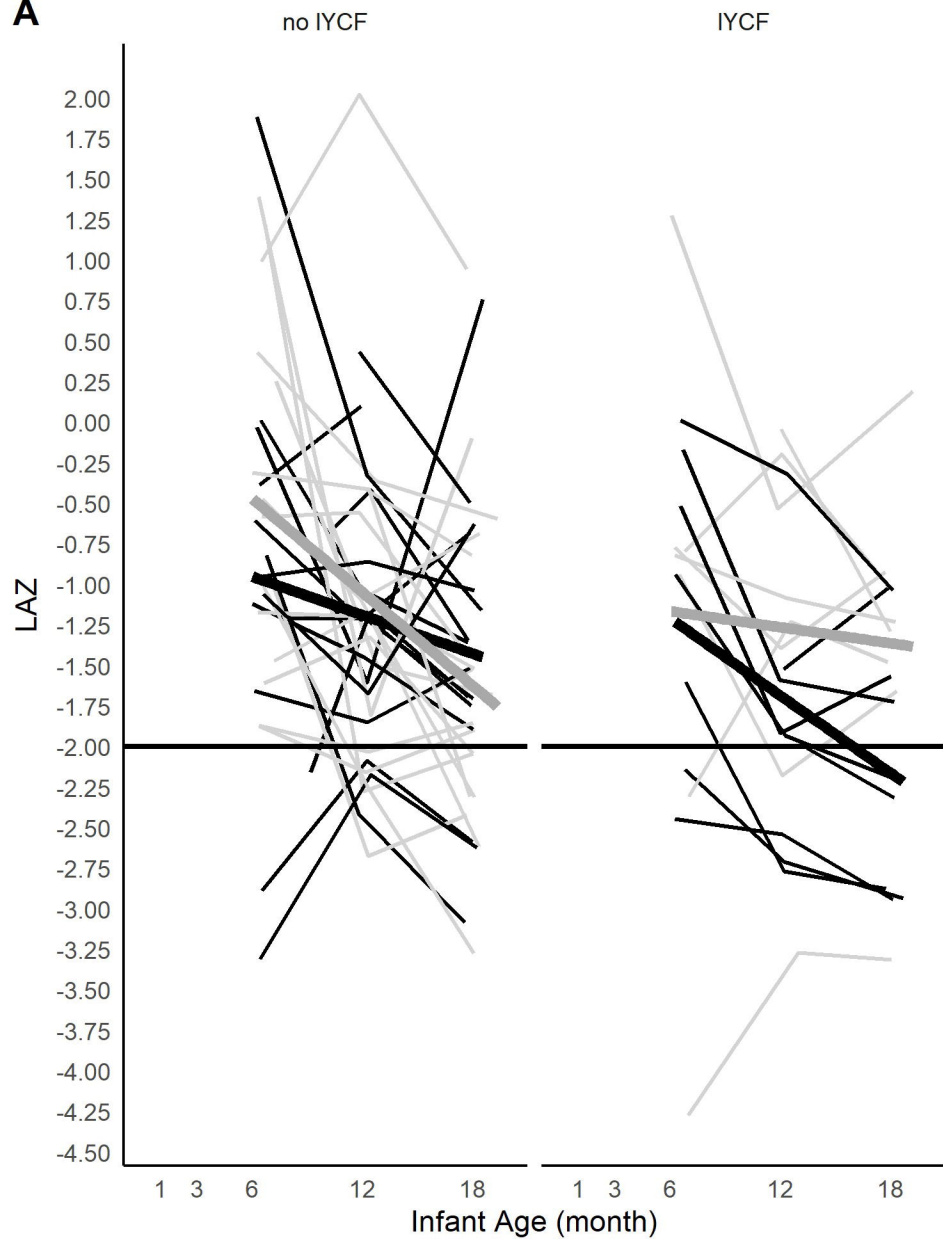


**B**

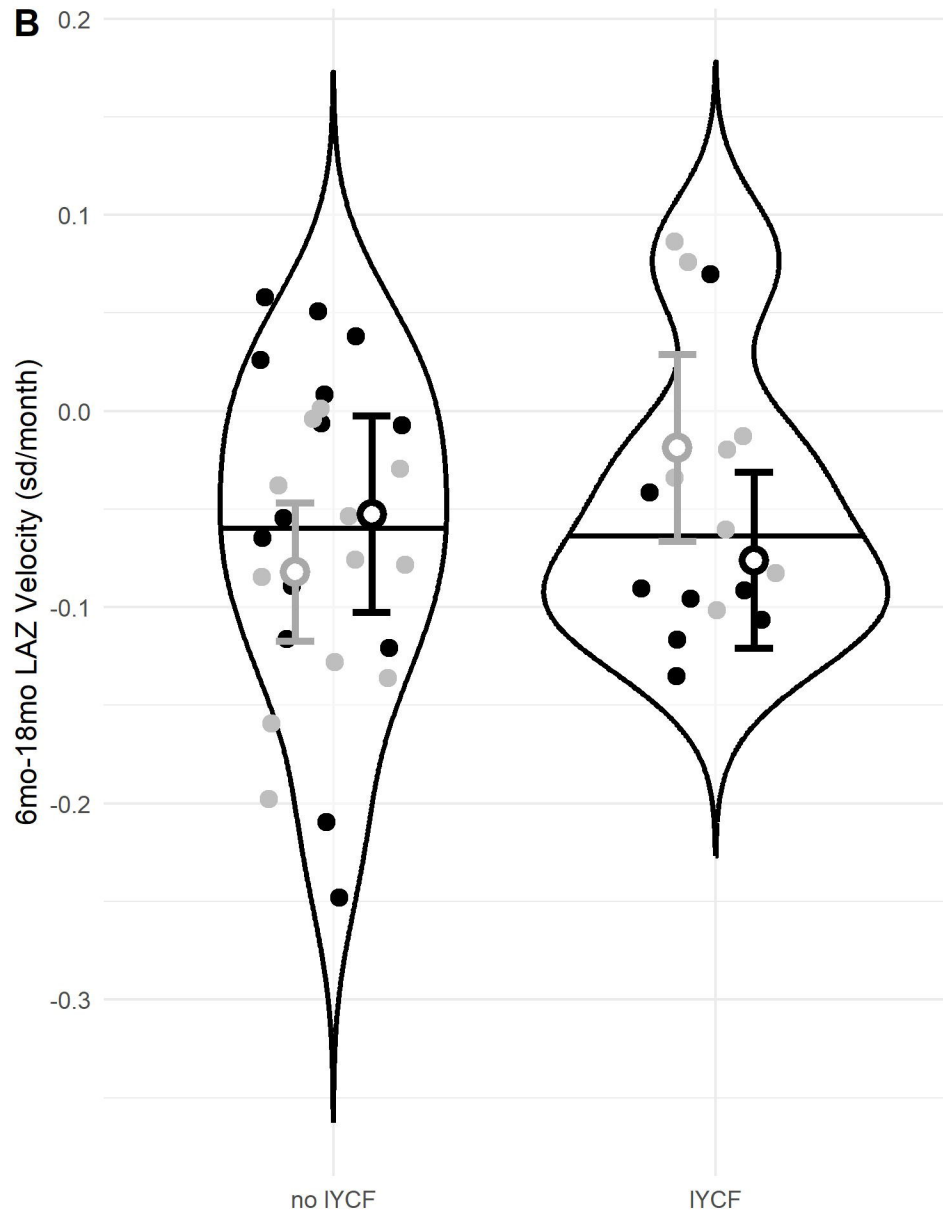


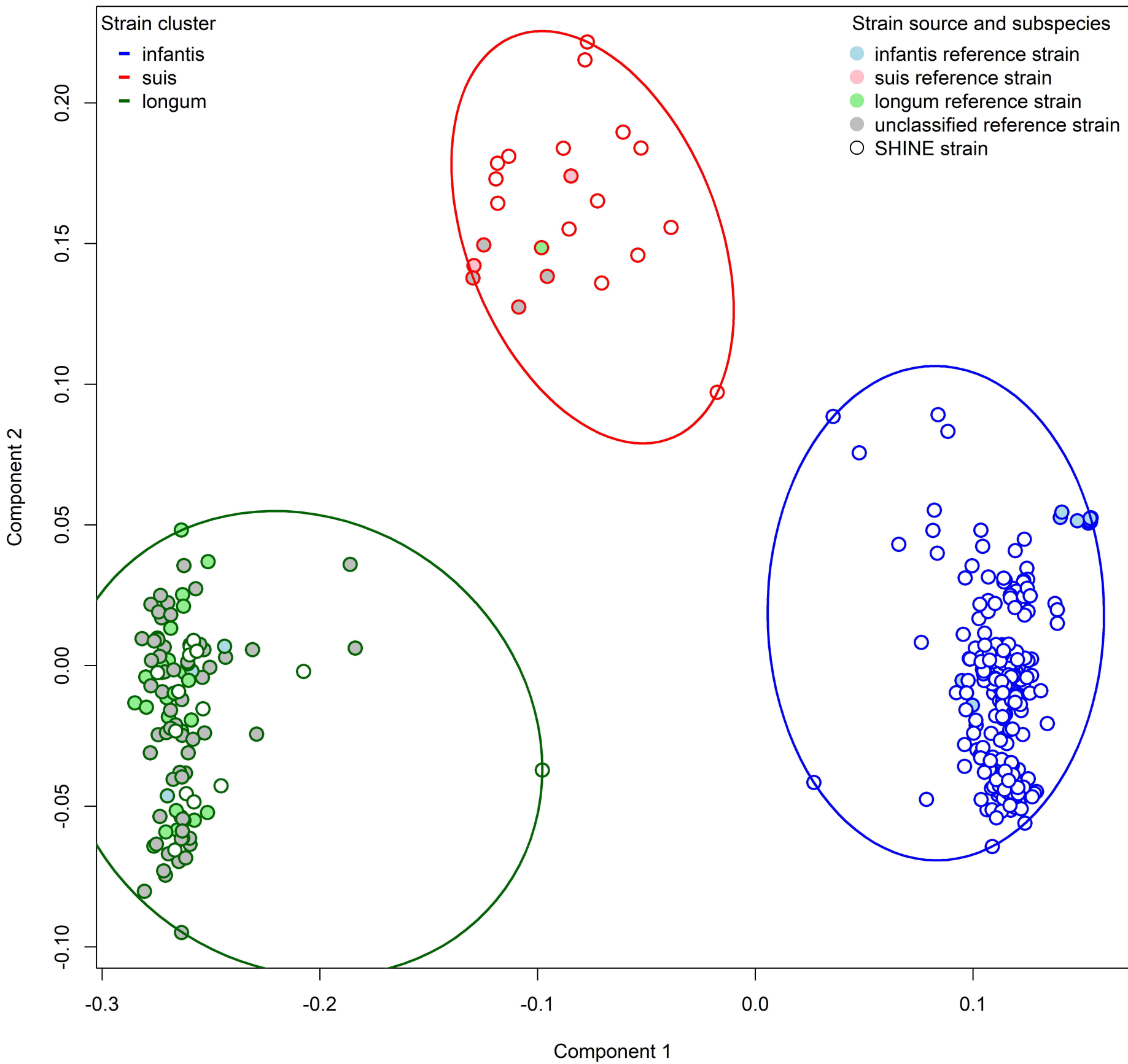
*B. longum* Rel. Ab. — Low — High

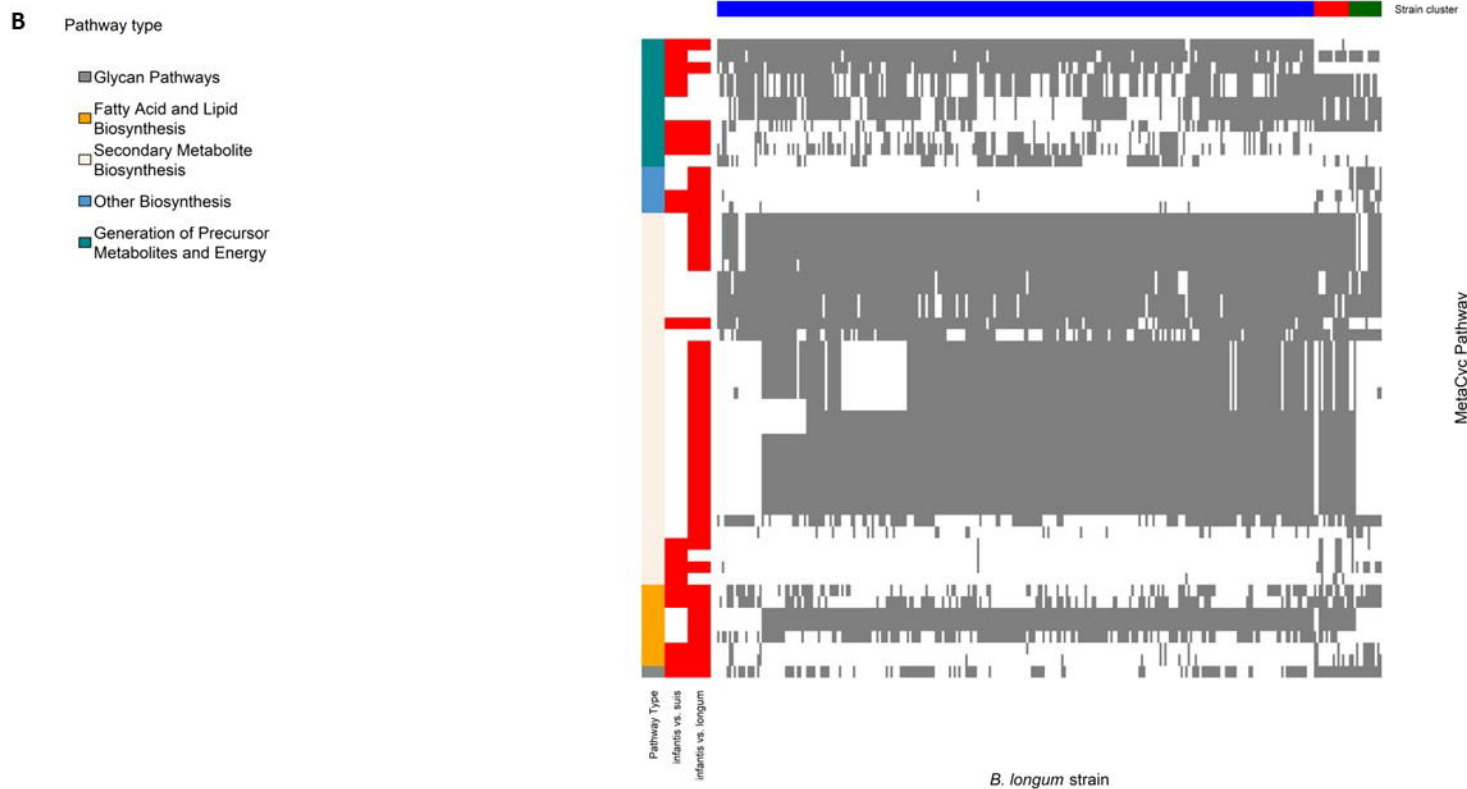
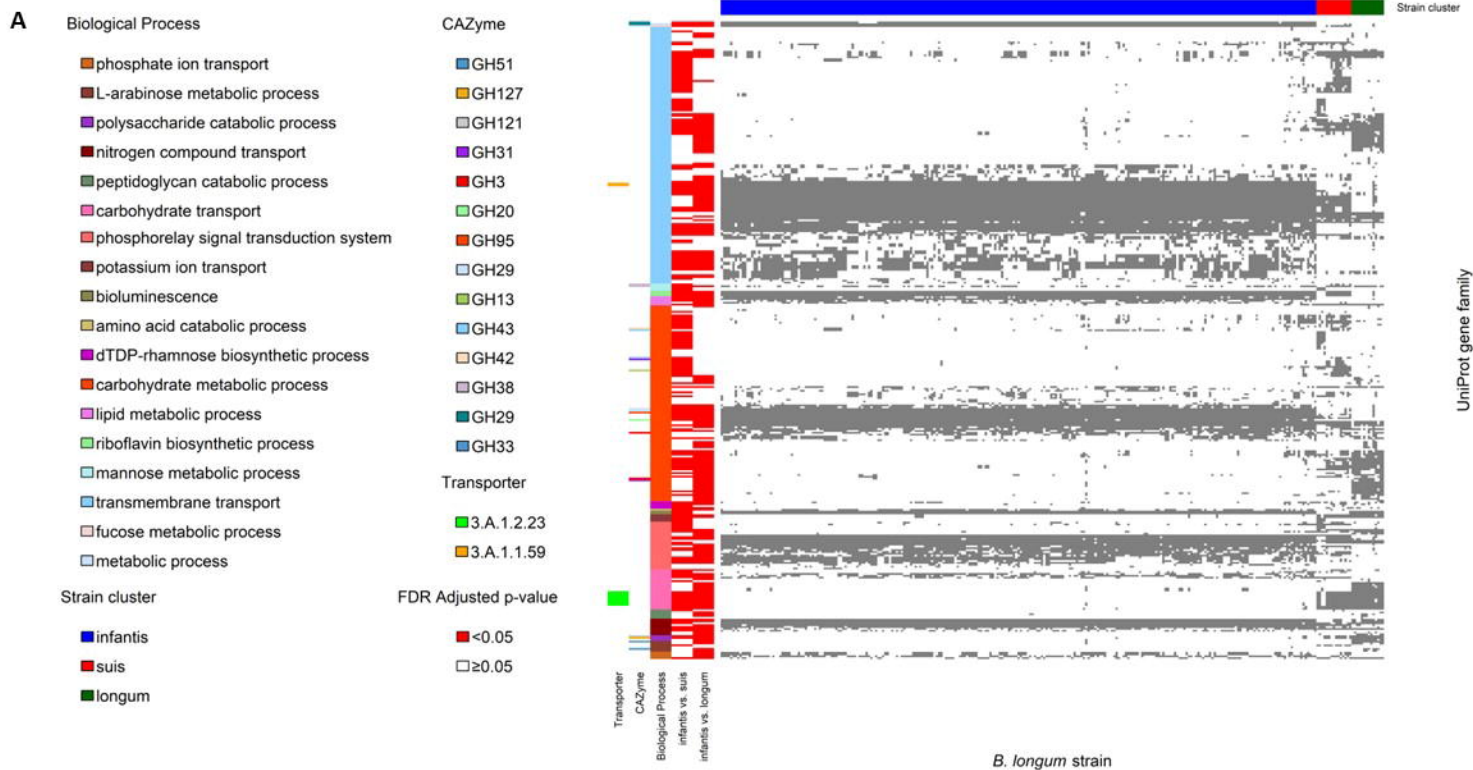
**A**



**B**

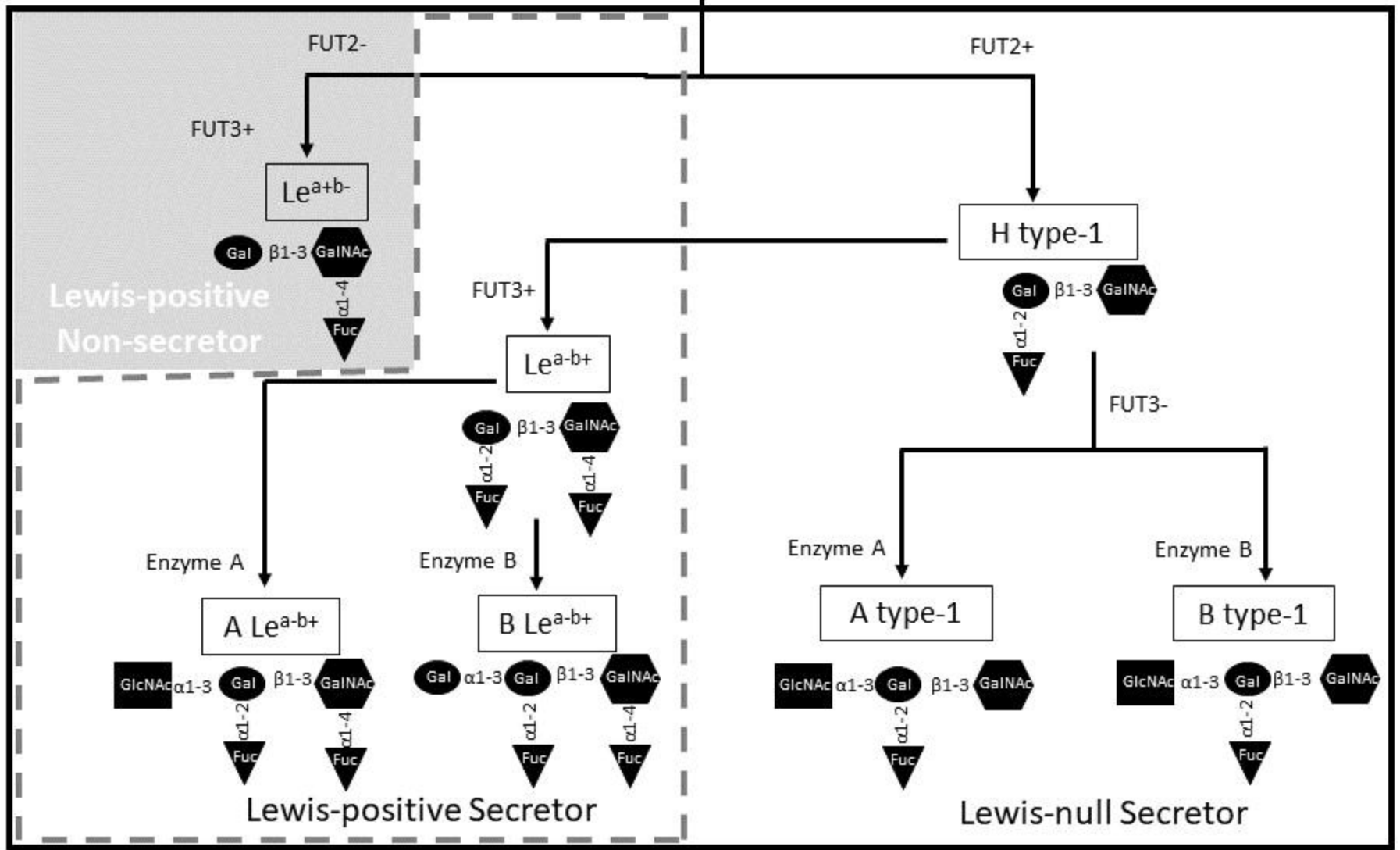






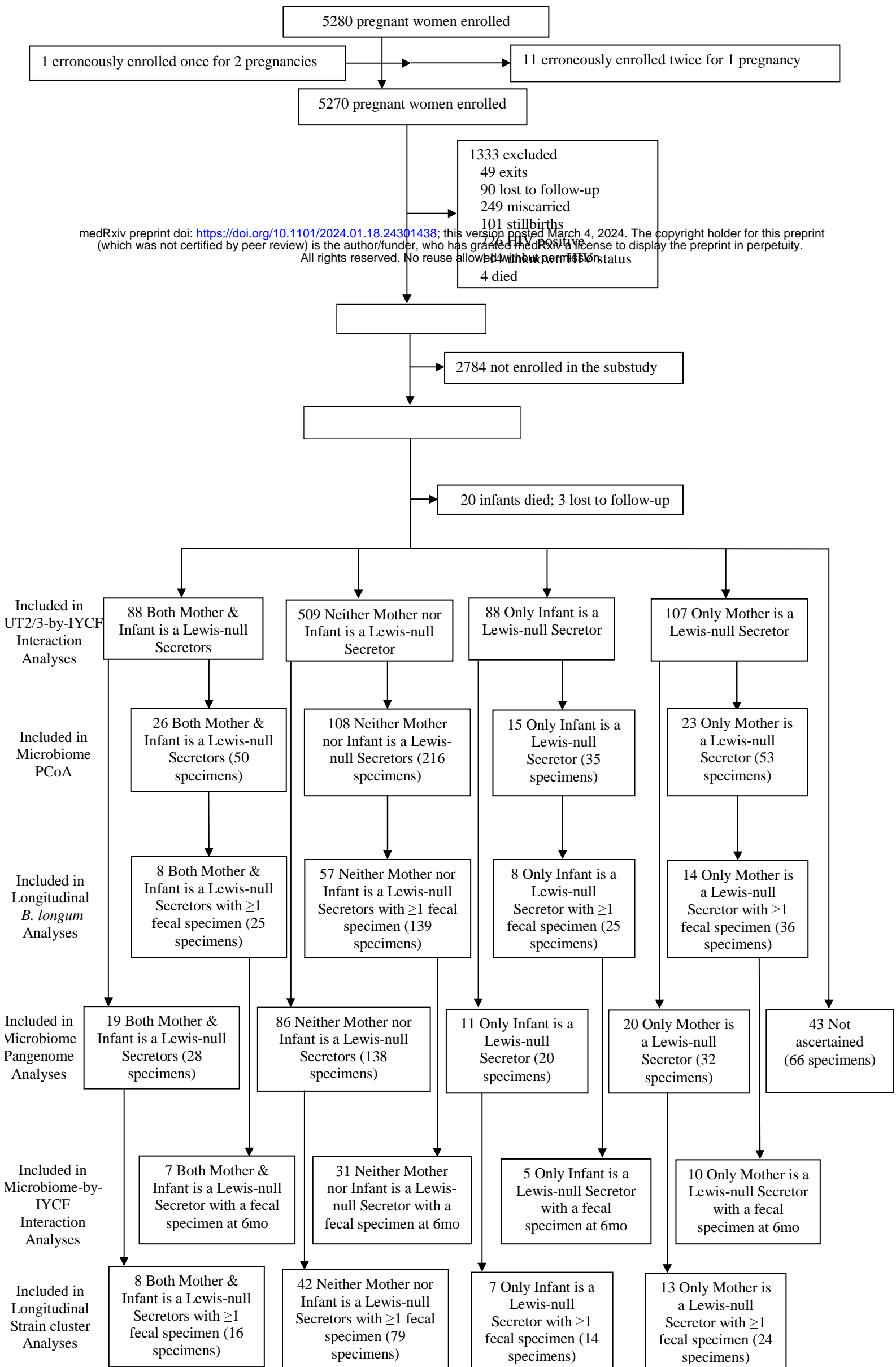


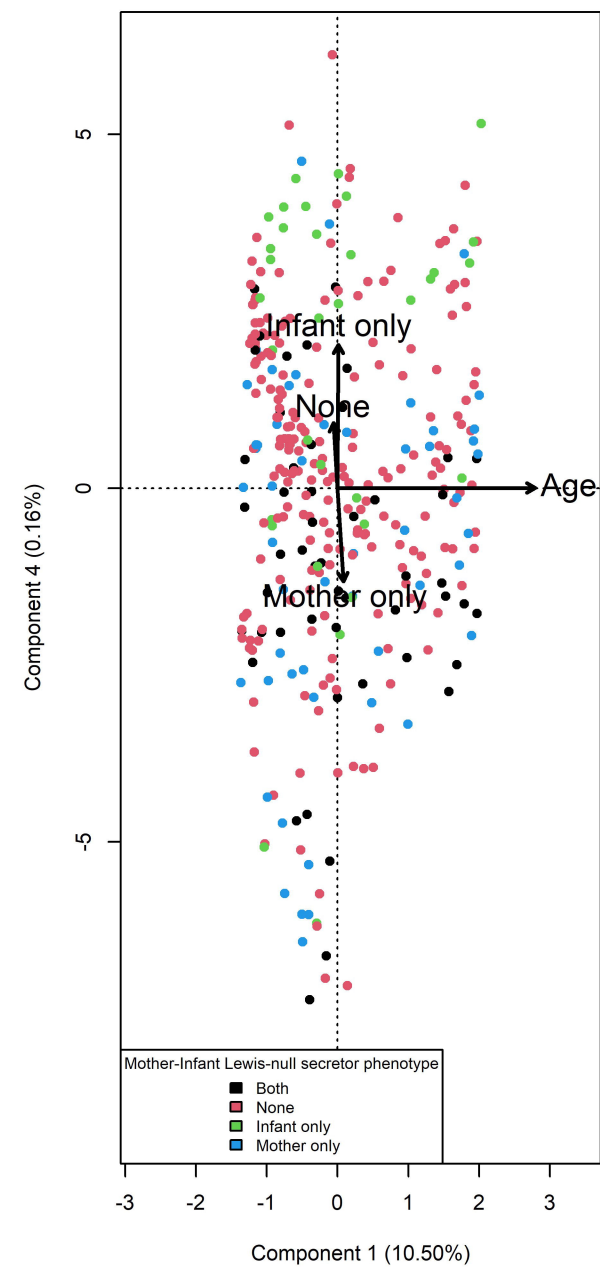
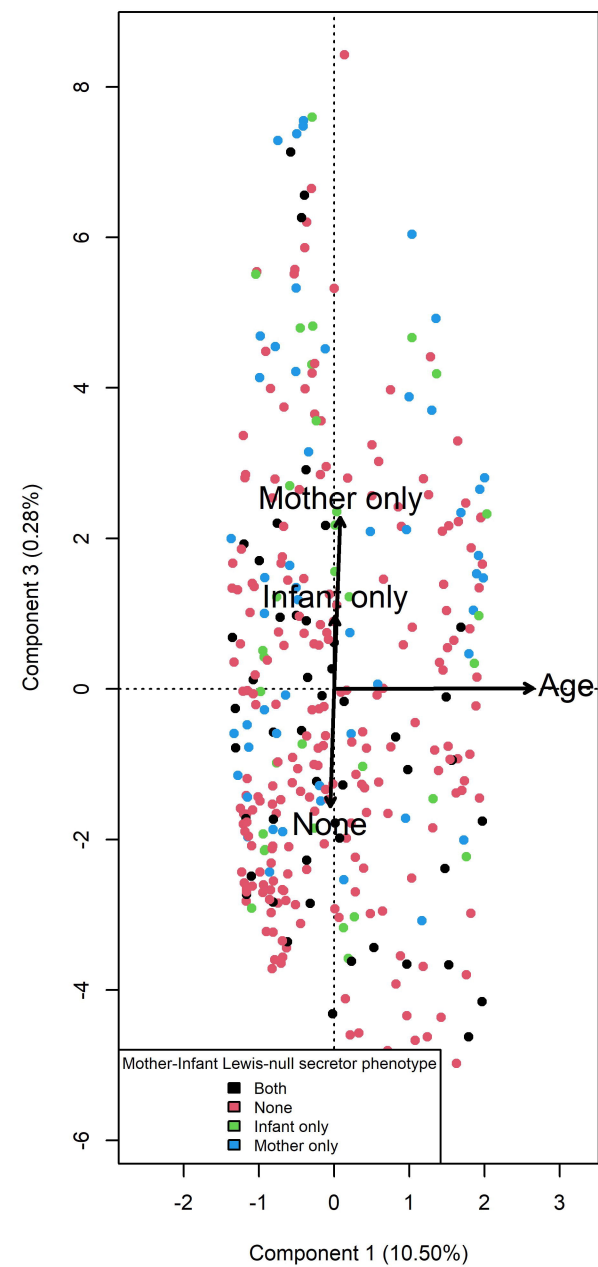
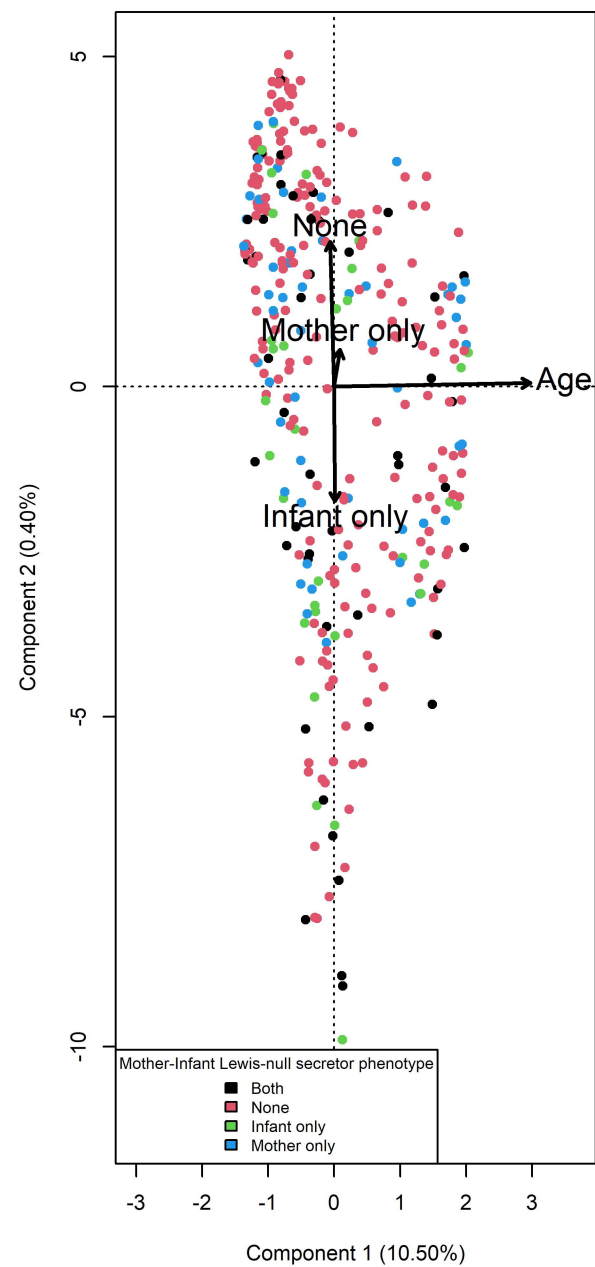
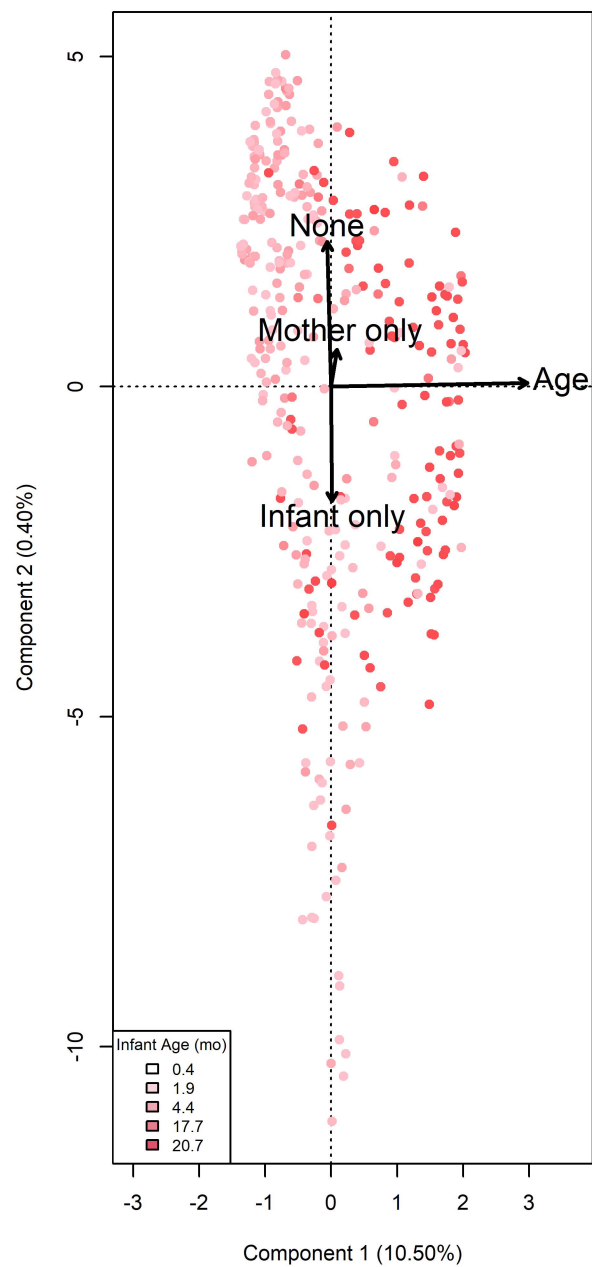
Type 1 Precursor

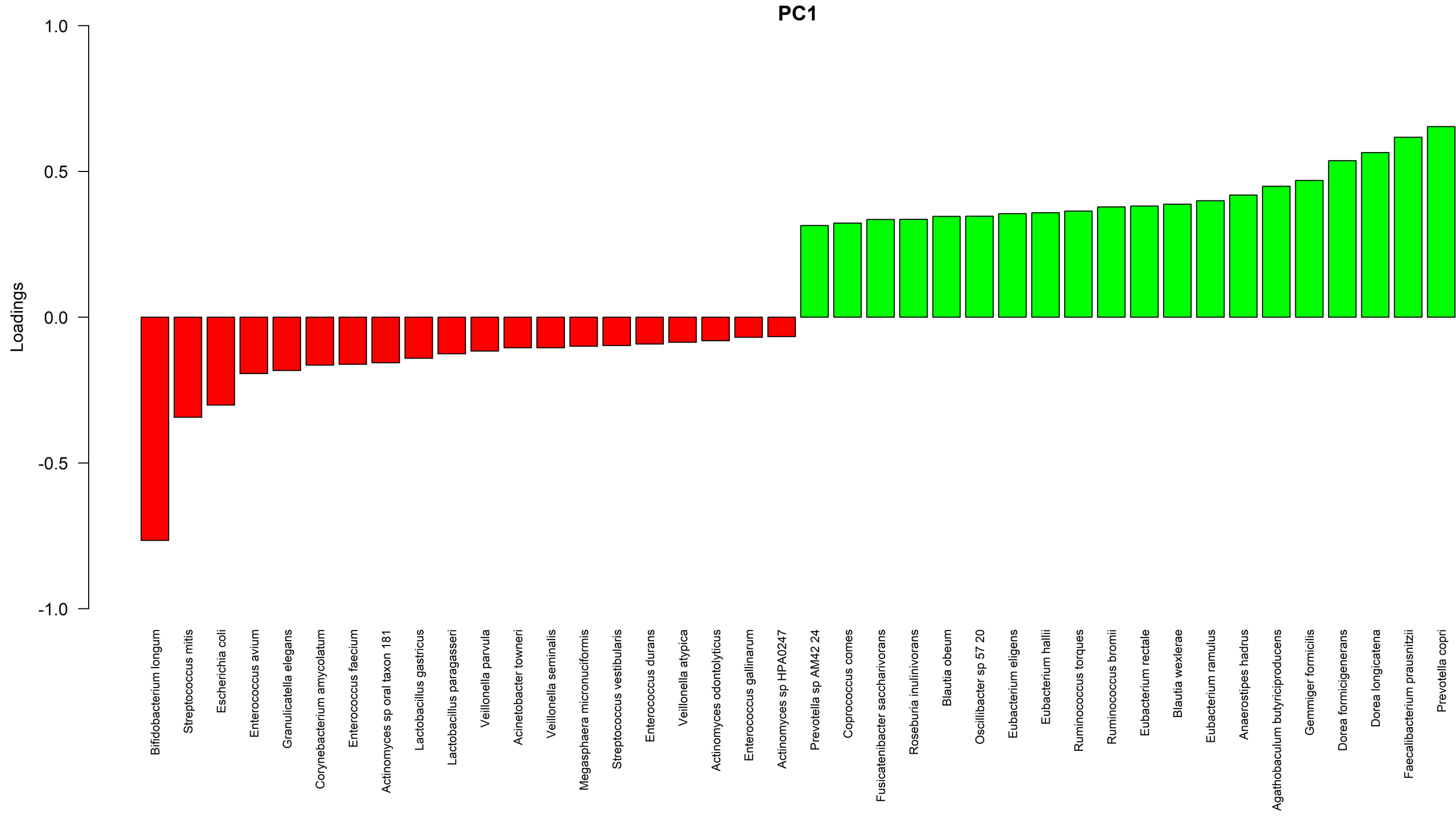


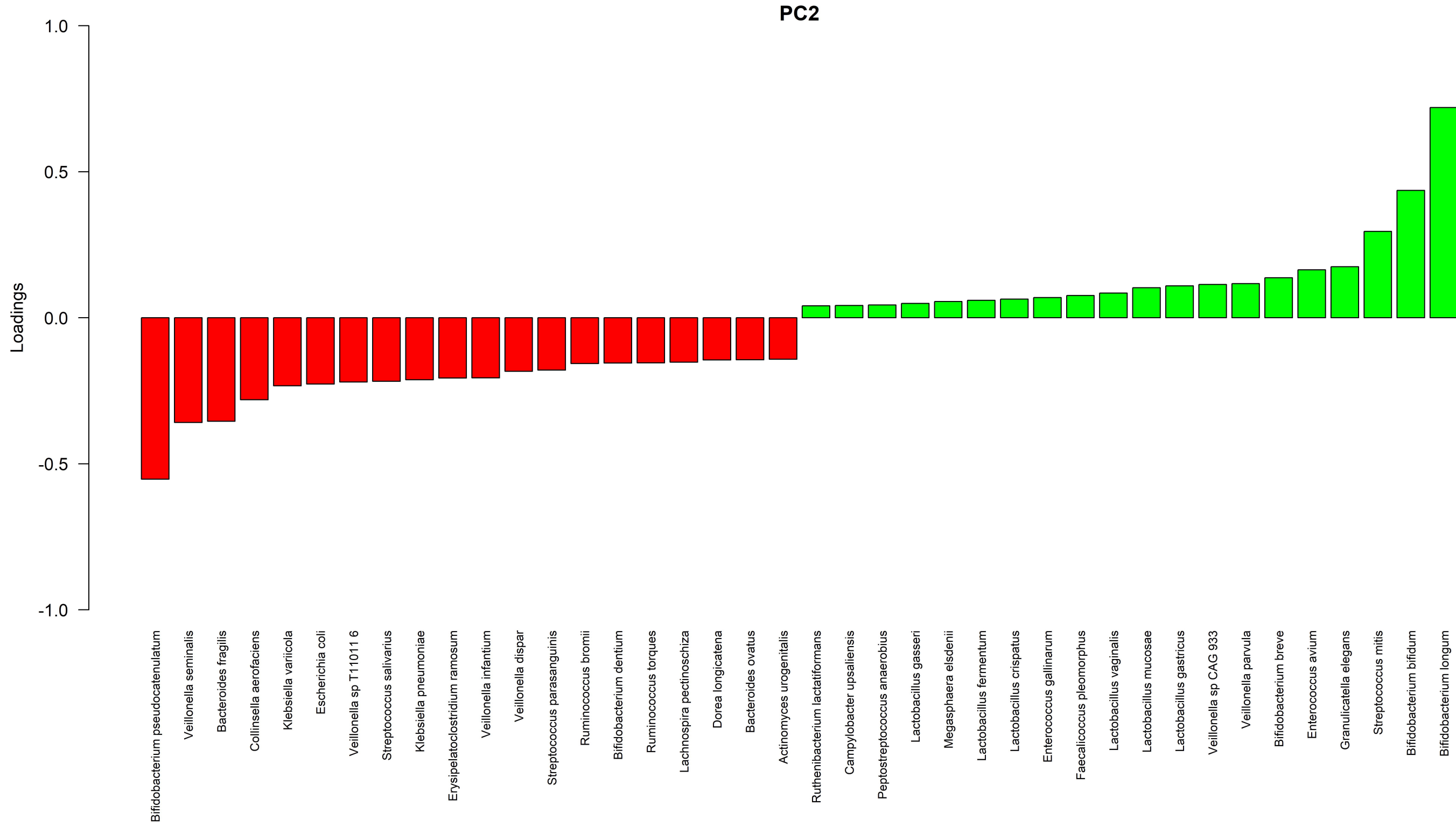
Legend:

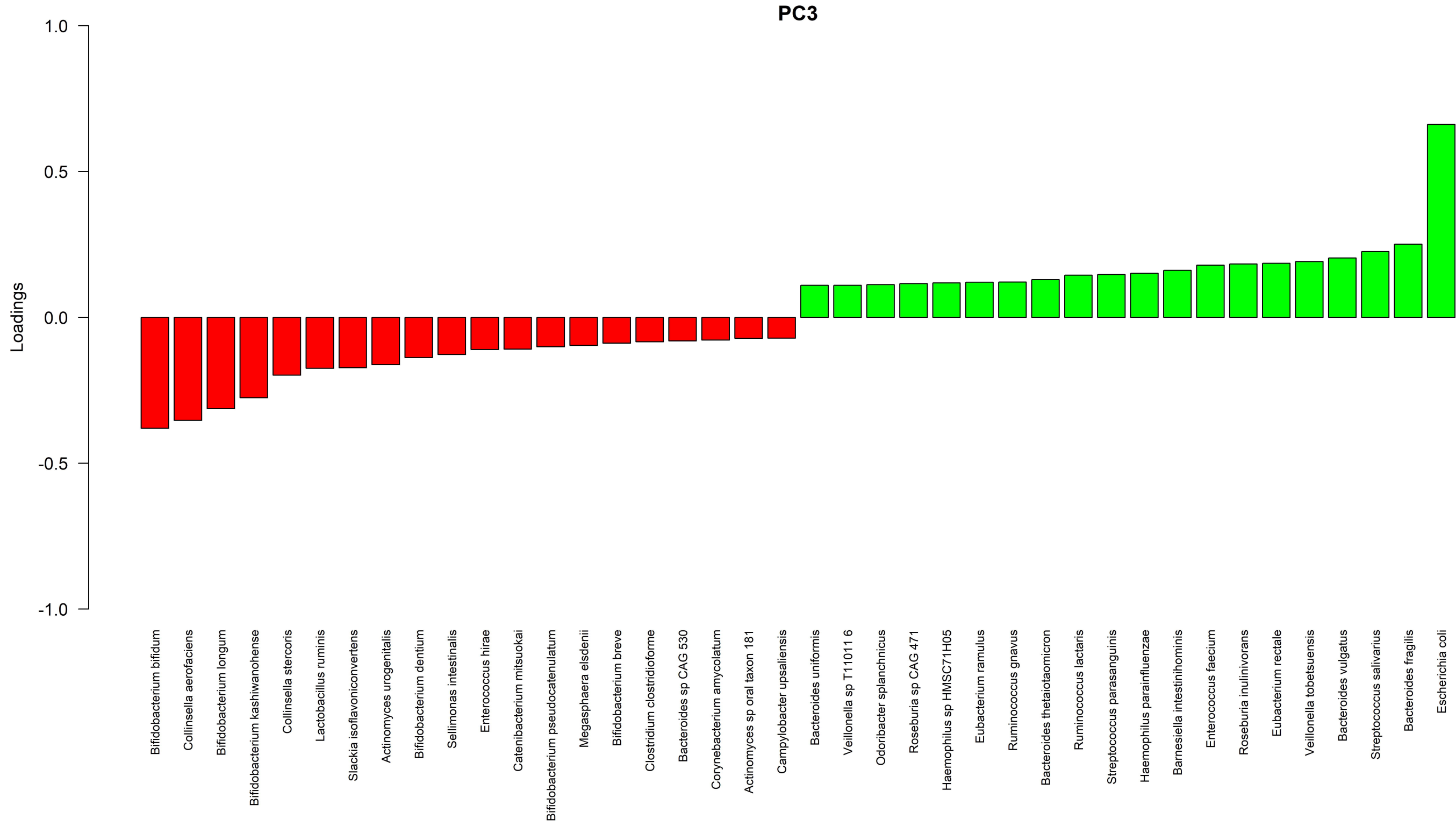
- Gal: Galactose
- Fuc: Fucose
- GlcNAc: N-Acetyl Glucosamine
- GalNAc: N-Acetyl Galactosamine

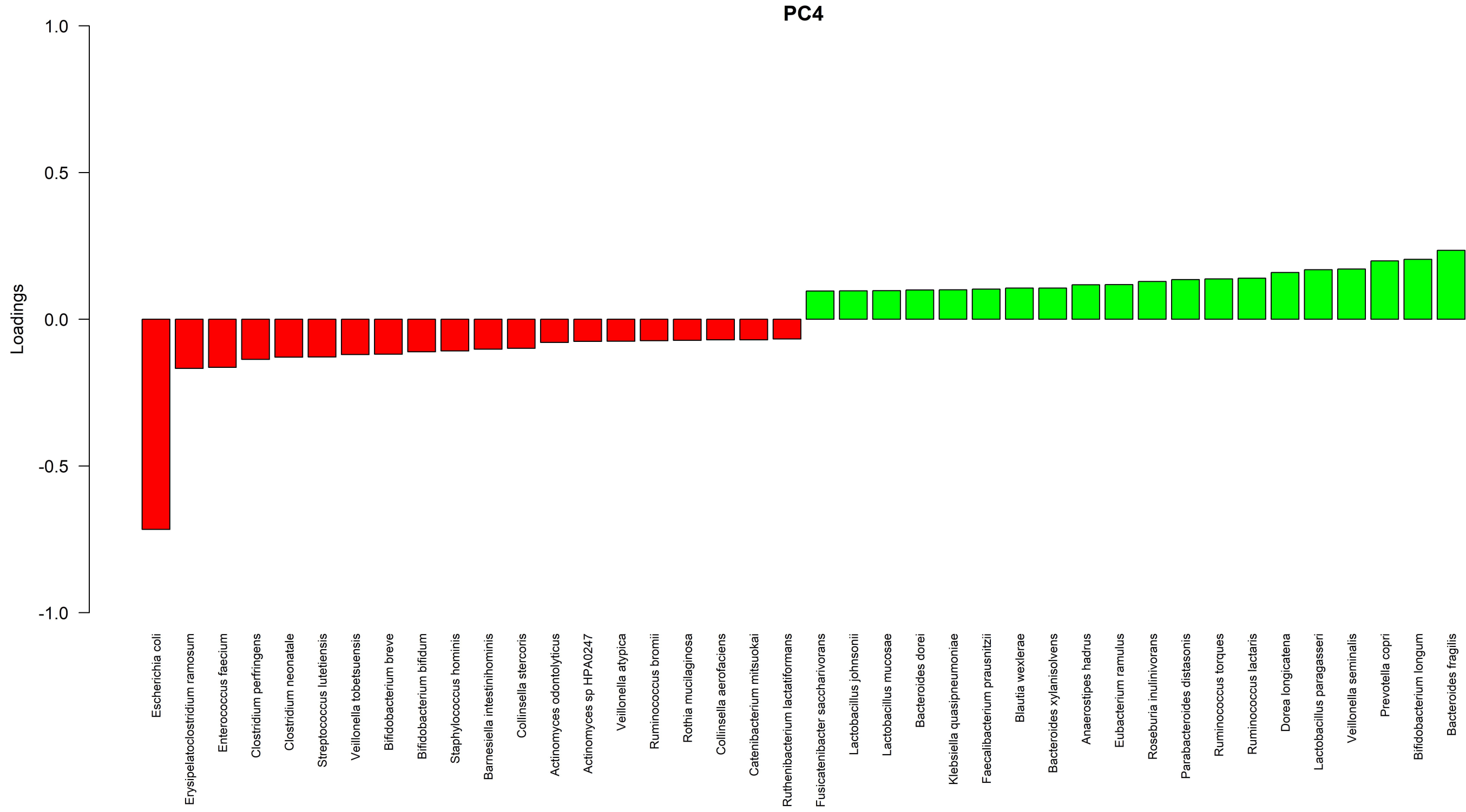














Reference subspecies

- longum
- infantis
- suis
- unclassified

Strain cluster

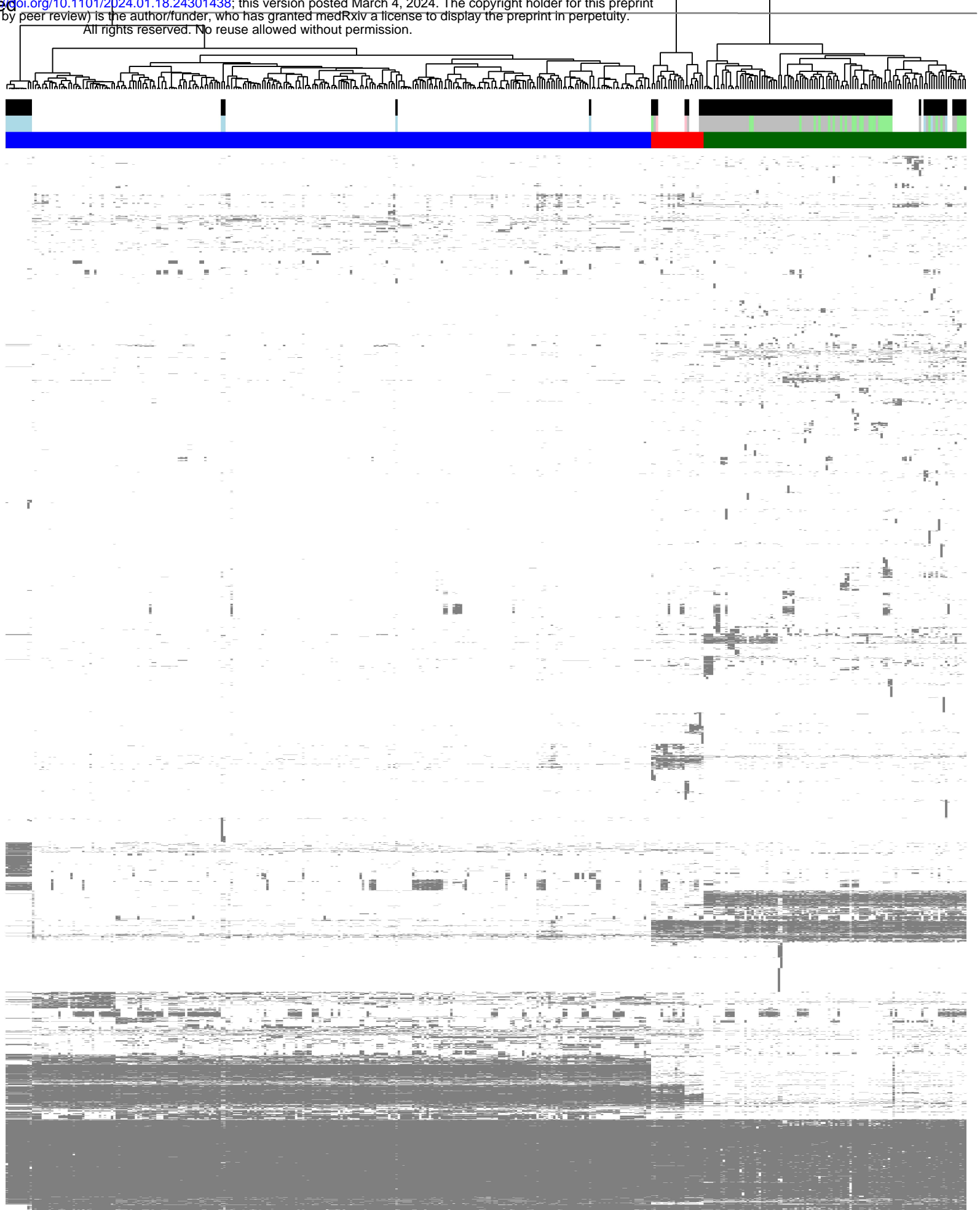
- infants
- suis
- longum

Strain source

- Reference strain
- SHINE strain

medRxiv preprint doi: <https://doi.org/10.1101/2024.01.18.24301438>; this version posted March 4, 2024. The copyright holder for this preprint (which was not certified by peer review) is the author/funder, who has granted medRxiv a license to display the preprint in perpetuity. All rights reserved. No reuse allowed without permission.

Strain source  
Reference subspecies  
Strain cluster



UniProt Gene Family

*B. longum* strain



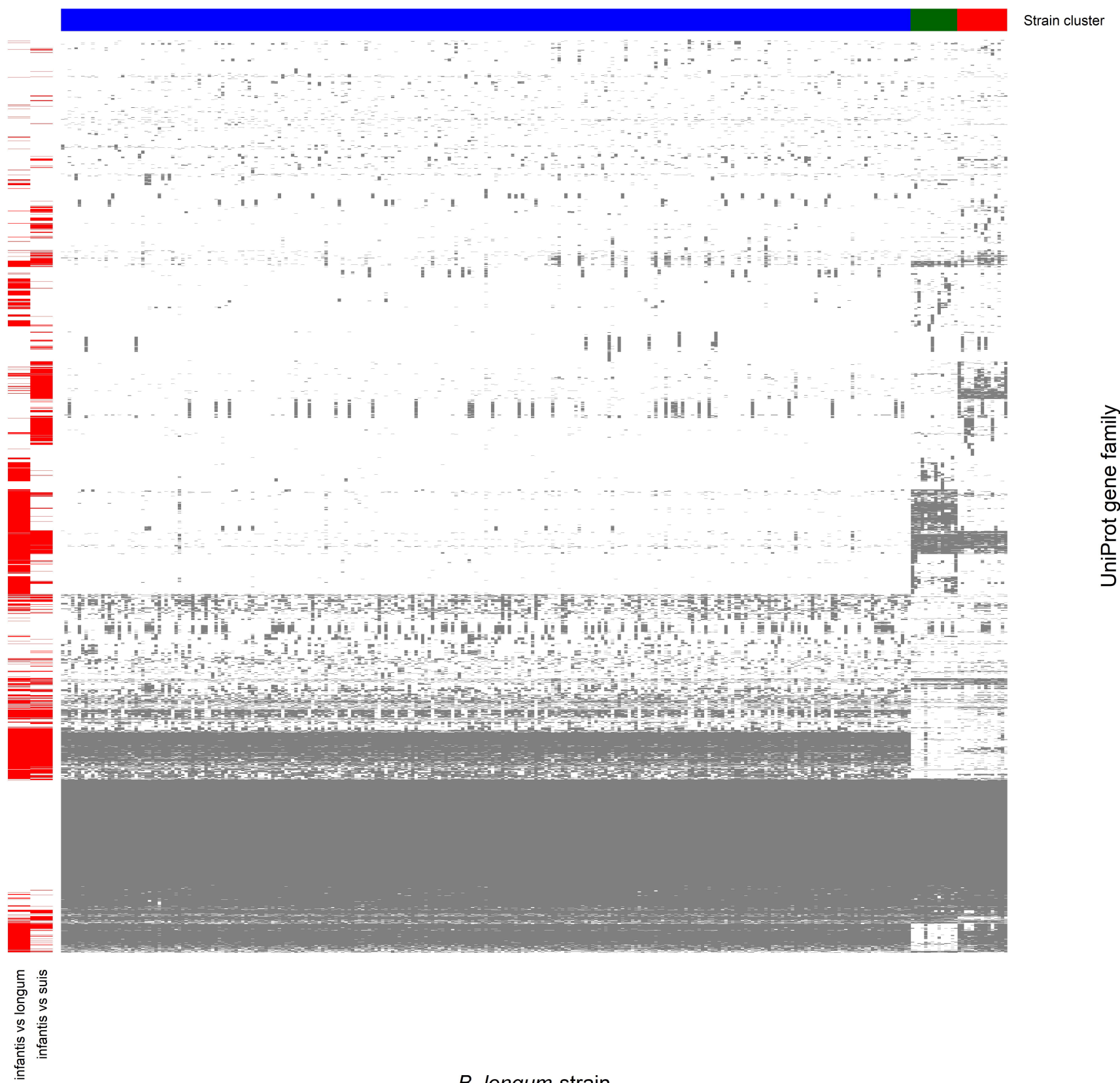
FDR Adjusted p-value

■ <0.05  
□ ≥0.05

Strain cluster

■ infantis  
■ suis  
■ longum

medRxiv preprint doi: <https://doi.org/10.1101/2024.01.18.24301438>; this version posted March 4, 2024. The copyright holder for this preprint (which was not certified by peer review) is the author/funder, who has granted medRxiv a license to display the preprint in perpetuity. All rights reserved. No reuse allowed without permission.



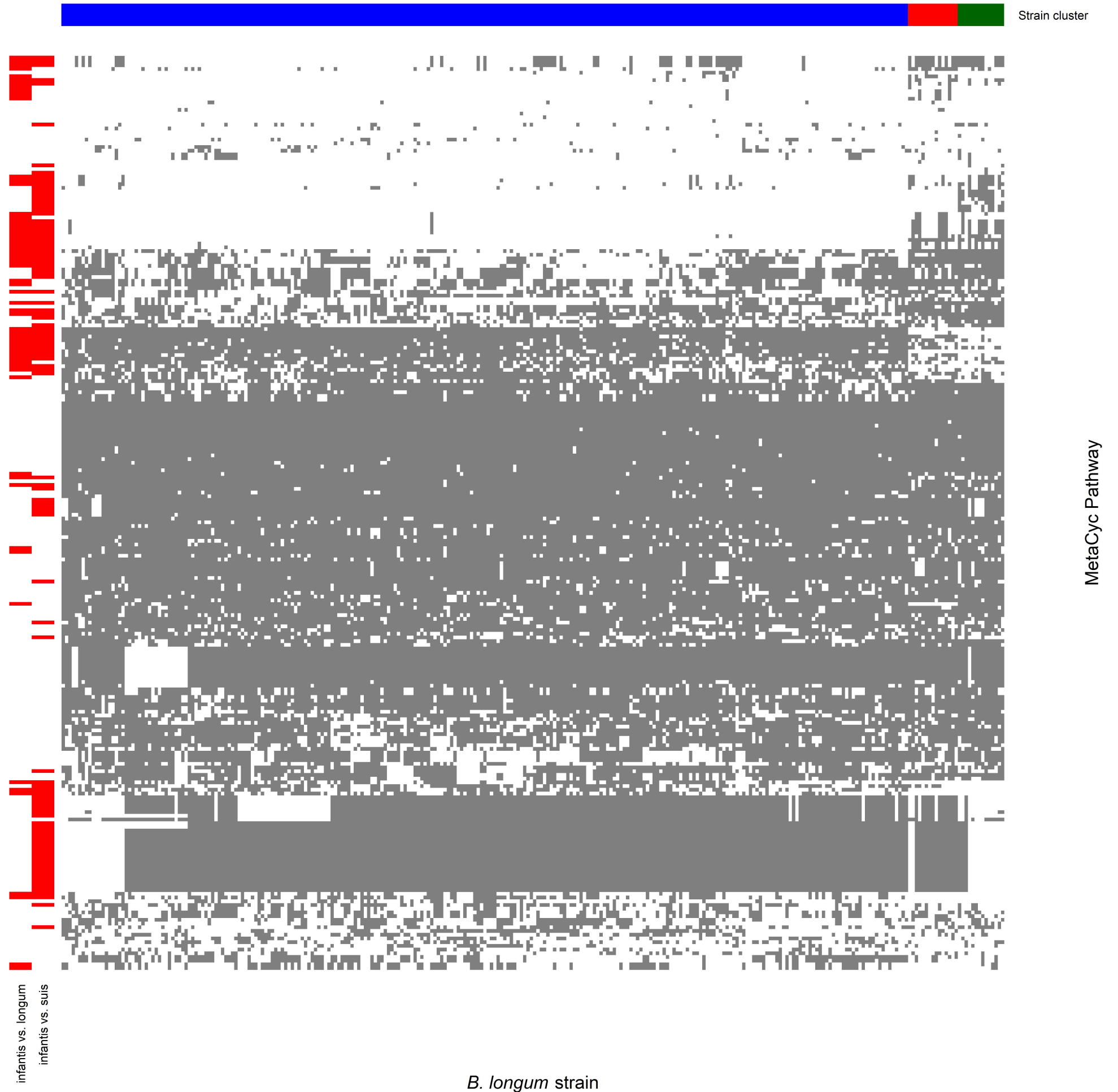
FDR Adjusted p-value

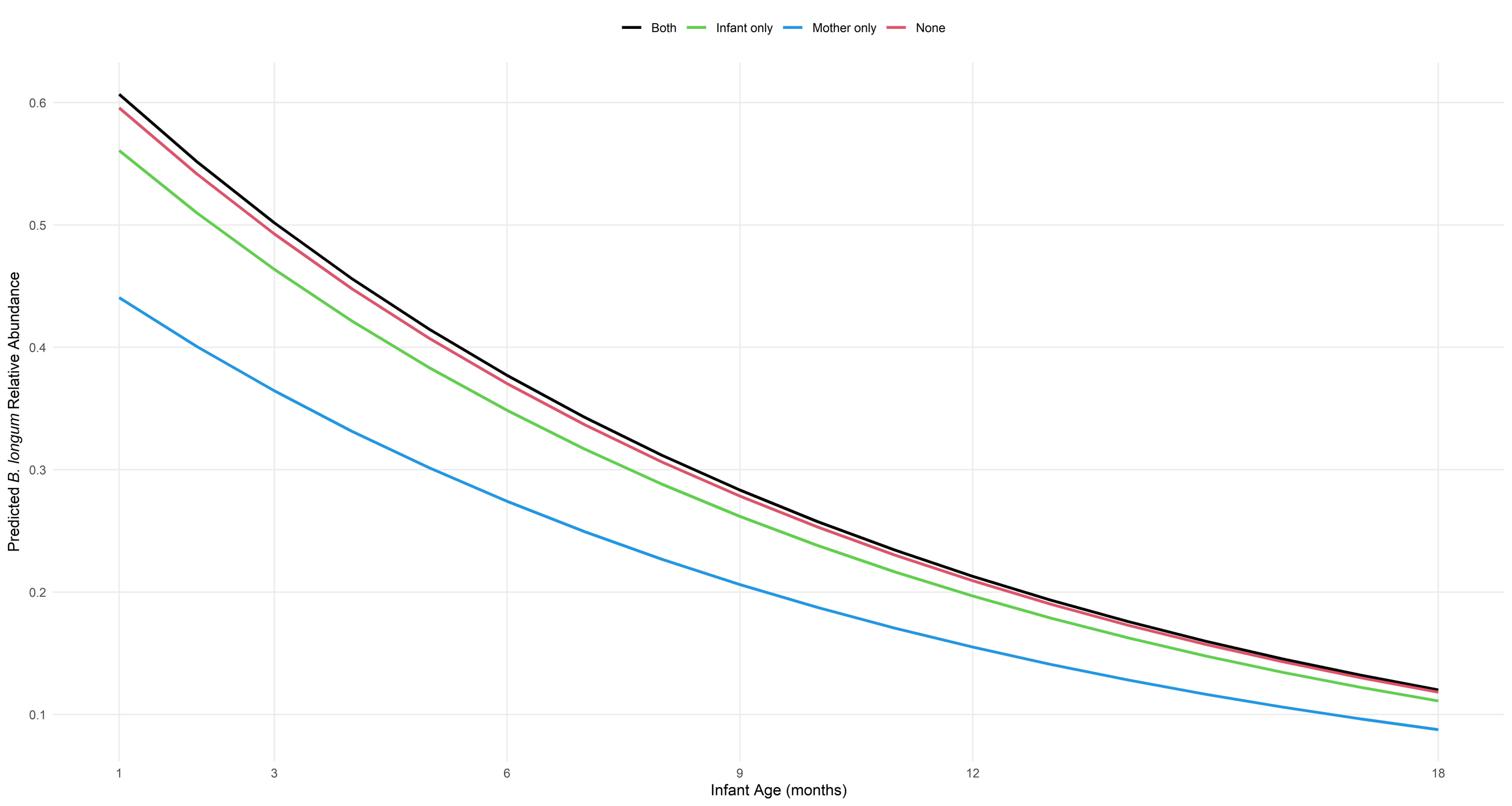
■ <0.05  
□ ≥0.05

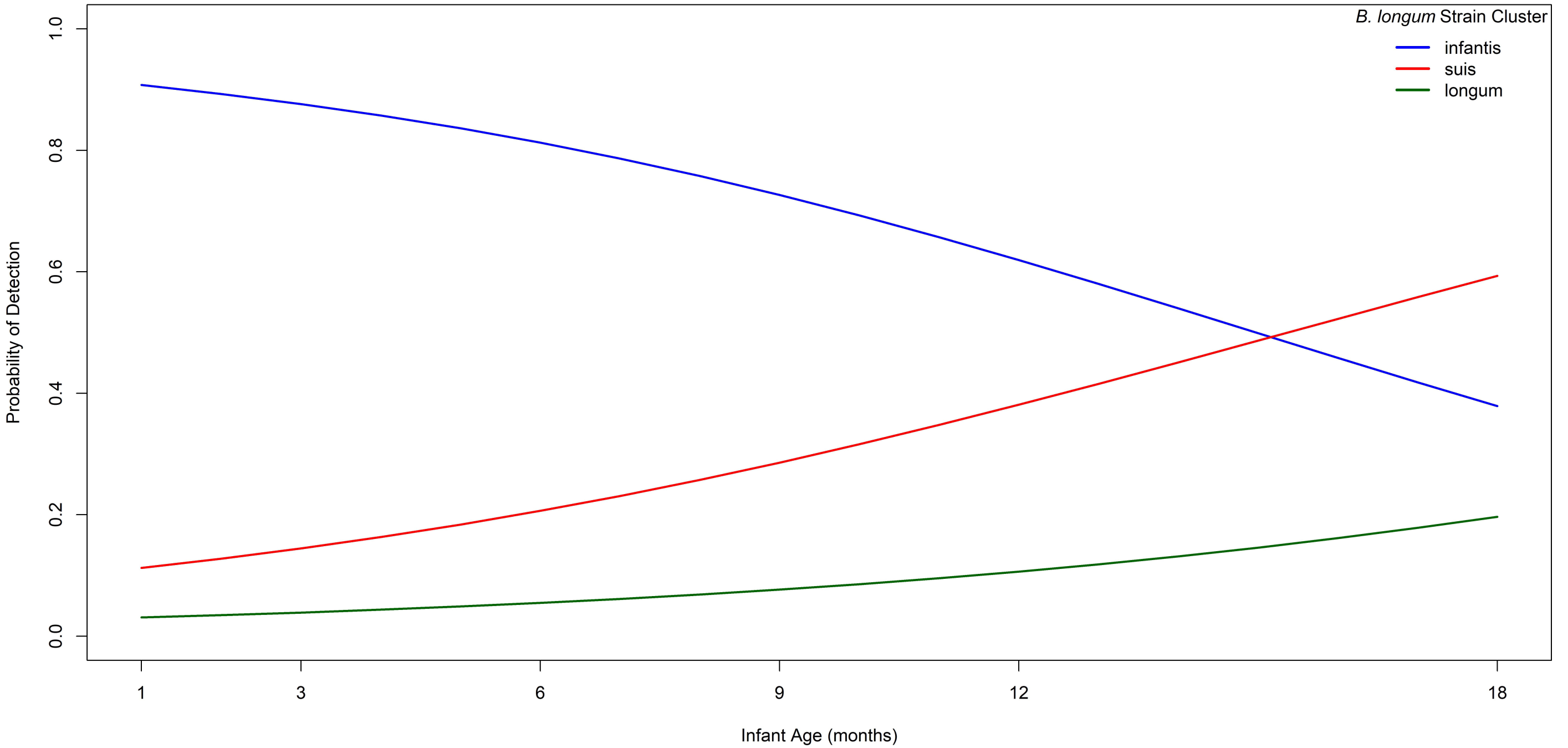
Strain cluster

■ infantis  
■ suis  
■ longum

medRxiv preprint doi: <https://doi.org/10.1101/2024.01.18.24301438>; this version posted March 4, 2024. The copyright holder for this preprint (which was not certified by peer review) is the author/funder, who has granted medRxiv a license to display the preprint in perpetuity. All rights reserved. No reuse allowed without permission.







— Both — None — Infant only — Mother only

